

NASA/CR-1999-209120/VOL5



# Acoustic Treatment Design Scaling Methods

## *Volume 5: Analytical and Experimental Data Correlation*

*W. E. Chien*  
*Rohr, Inc., Chula Vista, California*

*R. E. Kraft and A. A. Syed*  
*General Electric Aircraft Engines, Cincinnati, Ohio*

National Aeronautics and  
Space Administration

Langley Research Center  
Hampton, Virginia 23681-2199

Prepared for Langley Research Center  
under Contract NAS3-26617, Task 25

---

April 1999

---

Available from:

NASA Center for AeroSpace Information (CASI)  
7121 Standard Drive  
Hanover, MD 21076-1320  
(301) 621-0390

National Technical Information Service (NTIS)  
5285 Port Royal Road  
Springfield, VA 22161-2171  
(703) 605-6000

## Abstract

The primary purpose of the study presented in this volume of the Task Order 25 Final Report is to present the results and data analysis of the in-duct transmission loss measurements that were taken in the GEAE Acoustic Laboratory and analyzed by Rohr, Inc. Transmission loss testing was performed on full scale, 1/2 scale, and 1/5 scale treatment panel samples. The objective of the study was to compare predicted and measured transmission loss for full scale and sub-scale panels in an attempt to evaluate the variations in suppression between full and sub-scale panels which were ostensibly of equivalent design. A computer program was written to solve for the forward and backward mode coefficients of acoustic propagation in a rectangular duct based on pressure measurements in hardwall sections of the duct.

Modal measurement data taken at GEAE were transferred to Rohr, Inc, for analytical evaluation. Using a modal analysis duct propagation prediction program, Rohr compared the measured and predicted mode content. Generally, the results indicate an unsatisfactory agreement between measurement and prediction, even for full scale. This is felt to be attributable to difficulties encountered in obtaining sufficiently accurate test results, even with extraordinary care in calibrating the instrumentation and performing the test. Test difficulties precluded the ability to make measurements at frequencies high enough to be representative of sub-scale liners.

It is concluded that transmission loss measurements without ducts and data acquisition facilities specifically designed to operate with the precision and complexity required for high sub-scale frequency ranges are inadequate for evaluation of sub-scale treatment effects. If this approach is to be pursued further, it will be necessary to develop adequate sub-scale laboratory test facilities and provide instrumentation of sufficient precision and complexity.



## Table of Contents

1. Introduction .....	1
2. Basic Theory of Flow Duct Acoustics .....	3
2.1 Sound Propagation in a Rectangular Duct with Flow .....	3
2.2 Governing Wave Equation in the Presence of Grazing Flow .....	6
2.3 Description of Hardwall and Softwall Boundary Conditions .....	7
2.3.1 Softwall Case .....	7
2.3.2 Hardwall Case .....	8
2.4 Numerical Solution of Eigenvalues .....	9
2.5 References for Section 2 .....	11
3. Modal Measurement Data Analysis .....	13
3.1 Modal Expansion .....	13
3.2 Matrix Formulation .....	16
3.3 Mode Coefficients by Least Squares Fit and Singular Value Decomposition .....	17
3.4 Acoustic Energy Flux in the Duct with Flow .....	19
3.5 References for Section 3 .....	20
4. Acoustic Modal Measurement .....	21
5. Correlation of Theory with Experiment .....	23
5.1 Introduction .....	23
5.2 Hardwall Case - No Mean Flow .....	24
5.3 Softwall Case - No Mean Flow .....	26
5.3.1 Impedance Analysis .....	27
5.3.2 Noise Attenuation Analysis .....	27
5.4 Softwall Case - Uniform Mean Flow .....	30
5.4.1 Grazing Flow Impedance Analysis .....	30
5.4.2 Noise Attenuation Analysis .....	31
6. Conclusions and Recommendations .....	34
7. Appendix A - RD2PMM Program User's Guide .....	35
7.1 Program Versions and Choice of Number of Modes in the Expansion .....	35
7.2 Program Input File .....	36
7.3 Program Output .....	38
7.4 Running the Programs .....	39
7.5 Sample Case .....	39
8. Appendix B - Calibration of the Acoustic Data Acquisition System .....	54
8.1 Introduction .....	54
8.2 Calibration of the Signal Conditioning Amplifiers and the Tape Recorder Systems .....	54
8.3 Relative Calibration of the Kulite Transducers .....	54
8.4 Amplitude Calibration .....	55
8.5 Relative and Amplitude Calibration of the Transducers, Signal Conditioning Amplifiers, and the Tape Recorder System .....	55
9. Appendix C - Procedure for the Reduction of the Flow Duct Acoustic Data .....	56
9.1 Introduction .....	56
9.2 Relative Calibrations Of A Transducer Array System .....	56

9.2.1	Relative Calibrations $X_{s_u}(i, 1, f)$ Of The Upstream Systems.....	57
9.2.2	Relative Calibrations $X_{s_d}(i, 1, f)$ Of The Downstream Systems.....	57
9.2.3	The Calibration Of The Transducers Relative To A Reference Transducer.....	58
9.2.3.1	Relative Calibration Of The 20 Upstream Transducers.....	58
9.2.3.2	Relative Calibration Of The 20 Downstream Transducers.....	59
9.2.4	Calculation Of The Total System Relative Calibrations.....	60
9.3	Reduction And Correction Of The Transducer Signals.....	61
9.3.1	Reduction Of The Recorded Data From The Up Stream Transducers.....	61
9.3.2	Reduction Of The Recorded Data From The Downstream Transducers.....	61
10.	Appendix D - DC Flow Resistance and Impedance Measurements with Grazing Flow	63
10.1	Measurement of Impedance with Grazing Flow by the Two-Microphone Method	63
10.2	DC Flow Tests with Grazing Flow.....	65
10.2.1	The Test Apparatus.....	65
10.2.2	Test Data.....	66

## 1. Introduction

The primary purpose of the study presented in this volume of the Task Order 25 Final Report is to present the results and data analysis of the in-duct transmission loss measurements that were taken in the GEAE Acoustic Laboratory and analyzed by Rohr, Inc. Transmission loss testing was performed on full scale, 1/2 scale, and 1/5 scale treatment panel samples. The objective of the study was to compare predicted and measured transmission loss for full scale and sub-scale panels in an attempt to evaluate the variations in suppression between full and sub-scale panels which were ostensibly of equivalent design.

The modal measurements consisted of acoustic pressure measurements at 20 microphone locations upstream and 20 locations downstream of the treatment sample. Partial arrays of microphones were used to obtain pressure-squared measurements of insertion loss, as well. The microphone positions for the upstream and downstream axial measurement locations varied with duct height and width. In addition to the height and width transverse mode decomposition, the two axial planes of measurement allow the separation of forward and backward travelling waves.

A schematic of the layout of the rectangular duct modal measurement test is shown in Figure (1-1). Tests were conducted at various frequencies and for various flow Mach numbers.

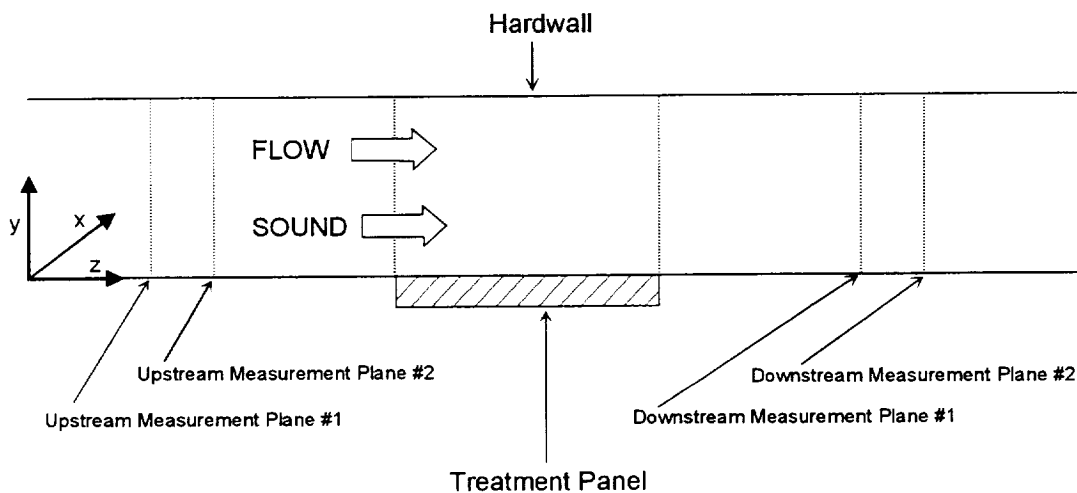


**Figure (1-1) Schematic of modal measurement rectangular duct.**

Modal measurements for a number of treatment panels were made in the Acoustic Laboratory Flow Duct Facility at GEAE. Descriptions of the test procedure, range of test conditions, and items tested are included below. A computer program was developed to perform the modal decomposition of the pressure measurements taken in the rectangular duct. A least squares best fit to the mode coefficients is obtained using the Singular Value Decomposition technique, which is a robust linear equation solver that identifies and overcomes possible ill-conditioning in the set of linear equations. A user's guide to the various versions of the program

is included, and some sample cases of use of the program for actual measured duct data is presented.

The modal measurement data taken at GEAE were transferred to Rohr, Inc, for analytical evaluation. Using a modal analysis duct propagation prediction program, Rohr compared the measured and predicted mode content. Descriptions of the modal analysis duct propagation prediction program, the comparative analysis procedure, and the results of the comparison are presented below.

Generally, the results indicate an unsatisfactory agreement between measurement and prediction, even for full scale. This is felt to be attributable to difficulties encountered in obtaining sufficiently accurate test results, even with extraordinary care in calibrating the instrumentation and performing the test. Test difficulties precluded the ability to make measurements at frequencies high enough to be representative of sub-scale liners.

It is concluded that transmission loss measurements without ducts and data acquisition facilities specifically designed to operate with the precision and complexity required for high sub-scale frequency ranges are inadequate for evaluation of sub-scale treatment effects. If this approach is to be pursued further, it will be necessary to develop adequate sub-scale laboratory test facilities and provide instrumentation of sufficient precision and complexity.

## 2. Basic Theory of Flow Duct Acoustics

### 2.1 Sound Propagation in a Rectangular Duct with Flow

Theoretical studies of sound propagation in an acoustically lined duct in the presence of grazing flow have been made by many investigators<sup>1,2,3,4,5</sup> (reference list included at the end of this Section). The derivation of the governing and boundary condition equations for this analysis is described in Sections 2.1, 2.2, and 2.3. The effect of an axially segmented wall impedance in a rectangular duct has been developed and studied previously by Eversman<sup>4</sup>, Kraft<sup>6</sup>, Bauer<sup>7</sup>, and Joshi<sup>8</sup>. The Finite Element Method (FEM) with Weighted Residual formulation<sup>9</sup> is used herein to resolve the eigenvalues and eigenvectors of the governing equation. This method has been successfully used to investigate the transmission of sound in a lined duct with flow by Eversman<sup>10</sup>, Astley<sup>10</sup>, and Vo<sup>11</sup>. The FEM formulation for this analysis is described in Section 2.4 using a three-node element and piece-wise quadratic shape functions.

The analytical model considered in this study is a rectangular duct with one or two lined side walls in the presence of a grazing flow. The geometry of the acoustically lined duct is illustrated in Figure (1-1). The fluid flow is assumed to be in z direction and is constant. The walls of the duct perpendicular to the y axis are treated with acoustic lining material, while the other two walls are not lined. The lining impedance (softwall boundary condition) is assumed to be uniform through the duct.

The objective is to calculate the attenuation of the sound wave as it propagates down a rectangular duct in the presence of flow. The equation of continuity of mass in vector notation is:

$$\frac{\partial \rho^*}{\partial t} + \nabla \cdot (\rho^* \vec{U}^*) = 0 \quad (2-1)$$

Euler's equation in the absence of body forces written as a single vector equation is:

$$\frac{\partial \vec{U}^*}{\partial t} + (\vec{U}^* \cdot \nabla) \vec{U}^* = -\frac{\nabla P^*}{\rho^*} \quad (2-2)$$

Because the acoustic processes are nearly adiabatic, the behavior of a perfect gas is described by the adiabatic equation of state:

$$\frac{P^*}{P_{\text{ref}}} = \left( \frac{\rho^*}{\rho_{\text{ref}}} \right)^\gamma \quad (2-3)$$

and

$$c = \sqrt{\frac{\partial P^*}{\partial \rho^*}} \quad (2-4)$$

The acoustic equations are obtained by considering a small perturbation  $(\rho, P, \vec{v})$  on a mean state  $(\rho_0, P_0, \vec{U}_0)$  so that

$$\rho^* = \rho_0 + \rho \quad (2-5)$$

$$P^* = P_0 + P \quad (2-6)$$

and

$$\vec{U}^* = \vec{U}_0 + \vec{v} \quad (2-7)$$

The resulting acoustic field equations are:

*Acoustic Continuity*

$$\frac{\partial \rho}{\partial t} + (\vec{U}_0 \cdot \nabla)\rho + \rho_0(\nabla \cdot \vec{v}) = 0 \quad (2-8)$$

*Acoustic Momentum*

$$\rho_0 \frac{\partial \vec{v}}{\partial t} + \rho_0(\vec{U}_0 \cdot \nabla)\vec{v} + \rho_0(\vec{v} \cdot \nabla)\vec{U}_0 + \rho(\vec{U}_0 \cdot \nabla)\vec{U}_0 = -\nabla P \quad (2-9)$$

These are the basic, first order, partial differential equations for the three unknown acoustic quantities:  $\rho$ ,  $P$ , and  $\vec{v}$ , where

$$\vec{v} = v_x \vec{i} + v_y \vec{j} + v_z \vec{k} \quad (2-10)$$

and

$$\vec{U}_0 = M(x, y) \vec{k} \quad (2-11)$$

The x, y, and z components of the acoustic momentum equation are:

$$\frac{\partial v_x}{\partial t} + M(x, y) \frac{\partial v_x}{\partial z} = -\frac{1}{\rho_0} \frac{\partial P}{\partial x} \quad (2-12)$$

$$\frac{\partial v_y}{\partial t} + M(x, y) \frac{\partial v_y}{\partial z} = -\frac{1}{\rho_0} \frac{\partial P}{\partial y} \quad (2-13)$$

and

$$\frac{\partial v_z}{\partial t} + v_x \frac{\partial M(x, y)}{\partial x} + v_y \frac{\partial M(x, y)}{\partial y} + M(x, y) \frac{\partial v_z}{\partial z} = -\frac{1}{\rho_0} \frac{\partial P}{\partial z} \quad (2-14)$$

## 2.2 Governing Wave Equation in the Presence of Grazing Flow

In order to simplify calculations, the variables used in Section 2.1 will be non-dimensionalized by the following parameters:

$$\begin{aligned}
 P &: \rho_0 c^2 \\
 \rho &: \rho_0 \\
 \bar{v} &: c \\
 \bar{U}_0 &: c \\
 x, y, \text{ and } z &: H \text{ (duct height)} \\
 t &: H/c
 \end{aligned} \tag{2-15}$$

After combining the acoustic continuity (Equation 2-8), momentum (Equation 2-9), and equation of state (Equations 2-3 and 2-4) equations with nondimensional variables (using original notation), only one equation with one unknown,  $P$ , will be generated:

$$\left( \frac{\partial}{\partial t} + M \frac{\partial}{\partial z} \right)^3 P + 2 \frac{\partial P}{\partial z} \left( \frac{\partial P}{\partial x} \frac{\partial M}{\partial x} + \frac{\partial P}{\partial y} \frac{\partial M}{\partial y} \right) = \left( \frac{\partial}{\partial t} + M \frac{\partial}{\partial z} \right) \nabla^2 P \tag{2-16}$$

where

$$P(x, y, z) = e^{i\eta t} e^{-ik_z z} P(x, y) \tag{2-17}$$

and  $\eta = \frac{2\pi f H}{c}$ ; (f: frequency Hz, c: speed of sound).

From Equation (2-17), we have

$$\frac{\partial P}{\partial t} = i\eta \quad \text{and} \quad \frac{\partial P}{\partial z} = -ik_z \tag{2-18}$$

Substituting Equation (2-18) into (2-16), and dividing (2-16) by  $-i\eta \left( 1 - M \frac{k_z}{\eta} \right)$ , yields:

$$\frac{\partial^2 \mathbf{P}}{\partial x^2} + \frac{\partial^2 \mathbf{P}}{\partial y^2} + \left[ \frac{2 \frac{k_z}{\eta}}{1 - M \frac{k_z}{\eta}} \left[ \frac{\partial M}{\partial x} \frac{\partial \mathbf{P}}{\partial x} + \frac{\partial M}{\partial y} \frac{\partial \mathbf{P}}{\partial y} \right] \right. \\ \left. + \left\{ \eta^2 \left[ \left( 1 - M \frac{k_z}{\eta} \right)^2 - \left( \frac{k_z}{\eta} \right)^2 \right] \right\} \right] \mathbf{P} = 0 \quad (2-19)$$

In the region of uniform mean flow,  $M(x,y)=\text{constant}$ ;  $\frac{\partial M}{\partial x} = \frac{\partial M}{\partial y} = 0$ .

Equation (2-19) can be reduced to the following equation:

$$\frac{\partial^2 \mathbf{P}}{\partial x^2} + \frac{\partial^2 \mathbf{P}}{\partial y^2} + \left\{ \eta^2 \left[ \left( 1 - M \frac{k_z}{\eta} \right)^2 - \left( \frac{k_z}{\eta} \right)^2 \right] \right\} \mathbf{P} = 0 \quad (2-20)$$

## 2.3 Description of Hardwall and Softwall Boundary Conditions

### 2.3.1 Softwall Case

The development of boundary conditions is based on the continuity of the particle displacement across a boundary layer. The facing sheet of the softwall and the fluid in the duct are regarded as separated by a vortex sheet. At the outer surface (free stream side) of the vortex sheet, the amplitudes of the particle displacement ( $\xi_y$ ) and particle velocity ( $v_y$ ) are related by the following equation:

$$v_y = \left( \frac{\partial}{\partial t} + M \frac{\partial}{\partial z} \right) \xi_y = (i\eta - iMk_z) \xi_y \quad (2-21)$$

The amplitude of the particle displacement at the inner surface of the vortex sheet (axial flow is zero) is written as:

$$v_w = \frac{\partial \xi_w}{\partial t} = i\eta \xi_w \quad (2-22)$$

We assume continuity of particle displacement across the boundary layer,

$$\xi_w = \xi_y \quad (2-23)$$

The acoustic impedance ( $Z$ ) and Admittance ( $A$ ) are determined as

$$Z = \frac{P}{v_w} = \frac{1}{A} \quad (2-24)$$

From the momentum equations (2-12 and 2-13), at the outer edge of the vortex sheet, we obtain:

$$-\frac{\partial P}{\partial y} = \left( \frac{\partial}{\partial t} + M \frac{\partial}{\partial z} \right) v_y = (i\eta - iMk_z) v_y \quad (2-25)$$

Substituting Equations (2-21), (2-22), (2-23) and (2-24) into equation (2-25), we get

$$\frac{\partial P}{\partial y} = -i\eta A \left( 1 - M \frac{k_z}{\eta} \right)^2 P \quad (2-26)$$

### 2.3.2 Hardwall Case

By the method of separation of variables, the solution of equation (2-16) can be rewritten based on Equation (2-17):

$$P(x, y) = \left( A e^{ik_x x} + B e^{-ik_x x} \right) \left( C e^{ik_y y} + D e^{-ik_y y} \right) \quad (2-27)$$

where  $k_x$  and  $k_y$  are wave constants, and A, B, C and D are arbitrary constants which can be determined from pertinent boundary conditions. It should be noted that both symmetrical and asymmetrical modes exist on the cross section (x-y plane) of the duct in both the x and y directions. In the x direction,

$$\frac{\partial P \left( \frac{W}{2}, y \right)}{\partial x} = 0 \quad (2-28)$$

for symmetrical modes, and

$$P \left( \frac{W}{2}, y \right) = 0 \quad (2-29)$$

for antisymmetrical modes.

It should be noted that the normal component of the particle velocity vanishes at the hardwall. The boundary condition at the hardwall is given by:

$$\left. \frac{\partial P(x, y)}{\partial x} \right|_{x=0} = 0 \quad \text{and} \quad \left. \frac{\partial P(x, y)}{\partial x} \right|_{x=W} = 0 \quad (2-30)$$

The boundary condition at the softwall is given by:

$$\left. \frac{\partial P(x, y)}{\partial y} \right|_{y=0} \neq 0 \quad \text{and} \quad \left. \frac{\partial P(x, y)}{\partial y} \right|_{y=H} \neq 0 \quad (2-31)$$

If the above boundary conditions are used, then solutions of the wave equation are written as follows

$$P(x, y) = 4AC \cos(k_x x) \cos(k_y y) \quad (2-32)$$

where

$$k_x = \frac{n\pi}{W}, \quad \text{and} \quad n = 0, 2, 4, 6, \dots \text{ for symmetrical modes, and}$$

$$n = 1, 3, 5, \dots \text{ for antisymmetrical modes.}$$

## 2.4 Numerical Solution of Eigenvalues

In this section, numerical solutions for Equation (2-19) for the case of a fully developed duct flow and a boundary layer near the walls are presented. In the present problem, the pressure amplitude function  $P(y)$  could be expanded in terms of a set of basis functions ( $\Phi_j$ ) in the form:

$$P(y) = \sum_{j=1}^n P_j \Phi_j(y) \quad (2-33)$$

where the basis functions are generated using a three-node element with quadratic shape functions. For a generalized element ( $-1 \leq \xi \leq 1$ ),  $P$  can be expressed by the following equation:

$$P(\xi) = \begin{bmatrix} N_1(\xi), N_2(\xi), N_3(\xi) \end{bmatrix} \begin{bmatrix} P_1 \\ P_2 \\ P_3 \end{bmatrix} \quad (2-34)$$

where,  $-1 \leq \xi \leq 1$ , and

$$\begin{aligned}
N_1(\xi) &= \frac{1}{2}\xi(\xi - 1) \\
N_2(\xi) &= -(\xi + 1)(\xi - 1) \\
N_3(\xi) &= \frac{1}{2}\xi(\xi + 1)
\end{aligned} \tag{2-35}$$

The resulting error function  $\varepsilon(y)$  of Equation (2-19) produced by the assumed solution, Equation (2-33), is forced to be orthogonal to each of the basis functions; thus,

$$\int_0^1 W(y)\varepsilon(y)dy = 0 \tag{2-36}$$

where  $W(y)$  is the weight function or test function

$$W(y) = \sum_{i=1}^N \beta_i \Phi_i(y) \tag{2-37}$$

For the *plug flow condition*, Equation (2-36) becomes:

$$\begin{aligned}
&\int_0^1 W(y)\varepsilon(y)dy = \\
&\int_0^1 W(y) \left\{ \frac{\partial^2 P}{\partial x^2} + \frac{\partial^2 P}{\partial y^2} + \left\{ \eta^2 \left[ \left( 1 - M \frac{k_z}{\eta} \right)^2 - \left( \frac{k_z}{\eta} \right)^2 \right] \right\} P \right\} dy = 0
\end{aligned} \tag{2-38}$$

Using the standard integration-by-parts and rearranging the equation yields:

$$\begin{aligned}
\int_0^1 W(y)\varepsilon(y)dy &= \left( \frac{k_z}{\eta} \right)^0 \left\{ \int_0^1 \left[ \frac{\partial P}{\partial y} \frac{\partial W}{\partial y} - \left( \eta^2 - \frac{n^2 \pi^2}{b^2} \right) PW \right] dy \right\} \\
&+ \left( \frac{k_z}{\eta} \right)^0 \left( i\eta \left( 1 - M \frac{k_z}{\eta} \right)^2 [A_1 W(1)P(1) + A_0 W(0)P(0)] \right) \\
&+ \left( \frac{k_z}{\eta} \right)^1 \left\{ \int_0^1 2M\eta^2 PW dy \right\} + \left( \frac{k_z}{\eta} \right)^2 \left\{ \int_0^1 \eta^2 (1 - M^2) PW dy \right\}
\end{aligned} \tag{2-39}$$

Because  $\beta_i$  are arbitrary, Equation (2-36) represents  $N$  equations to be satisfied by  $P_i$  rather than the single equation it appears to be. Therefore, we choose  $\beta_1 = 1$ ,  $\beta_i = 0$  for  $i \neq 1$  of

the first linear equation, and  $\beta_2 = 1$ ,  $\beta_i = 0$  for  $i \neq 2$  of the second linear equation. Continuing in this fashion, we arrive at the system of  $N$  linear equations for the  $N$  unknowns of  $P_j$ .

Substituting the assumed  $\beta_i$  along with Equations (2-33) and (2-36) into Equation (2-39), it becomes:

$$\left\{ \left( \frac{k_z}{\eta} \right)^2 [A] + \left( \frac{k_z}{\eta} \right)^1 [B] + \left( \frac{k_z}{\eta} \right)^0 [C] \right\} \{ \tilde{P} \} = 0 \quad (2-40)$$

Therefore, the axial propagation constants  $k_{zn}^+$  and  $k_{zn}^-$  and their corresponding eigenvectors  $\tilde{P}_n^+$  and  $\tilde{P}_n^-$  can be determined by Equation (2-38) for positive- and negative-traveling acoustic modes.

## 2.5 References for Section 2

- 
1. D. C. Pridmore-Brown, "Sound Propagation in a Fluid Flowing Through an Attenuating Duct" *J. of Fluid Mech.* **4**, p.393-406, March 1958.
  2. P. Mungur and M.L. Gladwell, "Acoustic Wave Propagation in a Sheared Fluid Contained in a Duct" *J. Sound Vib.* **9**(1), p.28-49, June 1968.
  3. E. J. Rice, "Propagation of Waves in an Acoustically Lined Duct with a Mean Flow", NASA SP-207, p.345-355, 1969.
  4. W. E. Eversman, "Theoretical Prediction of the Influence of Mach Number on Sound Attenuation in a Flow Duct", Boeing Co. Rep. D3-8002, 1969.
  5. S. H. Ko, "Sound Attenuation in Lined Rectangular Ducts with Flow and Its Application to the Reduction of Aircraft Engine Noise", *Journal of Acoustical Society of America* **50**, p.1418-1432, 1971.
  6. R. E. Kraft, "Theory and Measurement of Acoustic Wave Propagation in Multi-Segmented Rectangular Flow Duct.", Ph.D Dissertation, University of Cincinnati, June 1976.
  7. A. B. Bauer and M. C. Joshi, "Classification of Acoustic Modes in a Lined Duct", AIAA 80-1016, June 1980.
  8. M. C. Joshi, R.E. Kraft, and S.Y. Son, "Analysis of Sound Propagation in Annular Ducts with Segmented Treatment and Sheared Flow" AIAA 82-0123, Jan. 1982.

- 
9. E. B. Becker, G. F. Carey, and J. T. Oden, "Finite Element an Introduction Vol I", Prentice-Hall, Inc., 1981.
  10. R. J. Astley, and W. Eversman, "A Finite Element Formulation of the Eigenvalue Problem in Lined Ducts with Flow" J. Sound Vib. **65**(1) p.61-74, 1979.
  11. P. T. VO, and W. Eversman, "A Method of Weighted Residuals with Trigonometric Basis Functions for Sound Transmission in Circular Ducts" J. Sound Vib. **56**(2) p.243-250, 1978.

### 3. Modal Measurement Data Analysis

#### 3.1 Modal Expansion

An objective of this study was to develop a computer program to perform the modal decomposition of the pressure measurements taken in the rectangular duct. A least-squares best fit to the measured data is used as the basis of the data analysis. The program has the capability of determining the sensitivity of the measured mode coefficients to errors in the measured data.

Special features of this modal data analysis program are:

1. The capability of weighting the measured pressure at each sensor based on a known or estimated uncertainty in the reliability of the sensor. This is done through an input of the standard deviation of the sensor measurement, nominally set to 1.0 if the standard deviation is unknown. Setting the standard deviation of a given sensor to 2.0, for instance, would weight that sensor measurement by 0.5, etc.
2. A Singular Value Decomposition linear equation solver is used to solve the linear equations resulting from the least-squares fit. This is a robust solution technique that may give useful results even in cases where the equations are ill-conditioned.
3. A computation of the variance of the resulting mode coefficients is made. This is a measure of the goodness-of-fit (or accuracy) of the modal expansion to the input data. It could be used to evaluate different geometric arrangements of sensor arrays or effects of random error in the measured pressures on errors in the resulting coefficients (using a random error generation simulation).

The analysis is based on the standard modal decomposition of acoustic waves in a hardwall rectangular duct with uniform mean flow.<sup>1,2</sup> (References are listed at end of Section.) If the geometric triplet  $(x,y,z)$  denotes the coordinates of an arbitrary point in the interior of or on the walls of the duct, as defined in Figure (3-1), then we can write the coordinates of the  $j^{\text{th}}$  pressure measurement point as  $(x_j,y_j,z_j)$ .

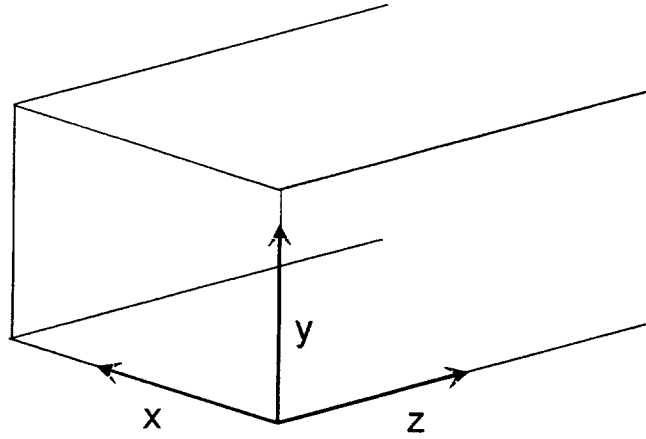


**Figure (3-1). Rectangular duct coordinate system conventions.**

In terms of the component rectangular duct modes, the pressure solution in the duct at the  $j^{\text{th}}$  measurement point is given by

$$p(x_j, y_j, z_j) = \sum_{m,n} \left[ CF_{mn} e^{i\kappa_{mn}^+ z_j} + CB_{mn} e^{i\kappa_{mn}^- z_j} \right] \cos\left(\frac{m\pi x_j}{W}\right) \cos\left(\frac{n\pi y_j}{H}\right) \quad (3-1)$$

where

- $m$  = mode order for x-modes ( $m = 0, 1, 2, \dots, \infty$ )
- $n$  = mode order for y-modes ( $n = 0, 1, 2, \dots, \infty$ )
- $W$  = duct width (x-direction)
- $H$  = duct height (y-direction)
- $CF_{mn}$  = mode coefficient for forward-travelling (m,n) mode
- $CB_{mn}$  = mode coefficient for backward-travelling (m,n) mode

The duct eigenvalues in the x- and y- directions are given by

$$m\pi/W \quad \text{and} \quad n\pi/H, \quad \text{respectively.}$$

In the hardwall duct, the eigenvalues are independent of mean flow.

The axial propagation constants, which do depend on mean flow, are given by

$$\kappa_{mn}^+ = \frac{-Mk + \sqrt{k^2 - (1 - M^2) \left[ \left( \frac{m\pi}{W} \right)^2 + \left( \frac{n\pi}{H} \right)^2 \right]}}{1 - M^2} \quad (3-2)$$

for the forward direction and by

$$\kappa_{mn}^- = \frac{-Mk - \sqrt{k^2 - (1 - M^2) \left[ \left( \frac{m\pi}{W} \right)^2 + \left( \frac{n\pi}{H} \right)^2 \right]}}{1 - M^2} \quad (3-3)$$

for the backward direction, where

- M = duct uniform flow Mach number
- k =  $\omega/c$  = wave number
- $\omega$  =  $2\pi f$  = circular frequency
- c = speed of sound
- f = frequency in Hertz.

Note that the eigenfunctions are the same in both directions, even in the flow case, whereas the propagation constants are different.

The acoustic pressure on the left side of Equation (3-1) is actually measured as a transfer function relative to one sensor chosen as the reference sensor. Thus the pressure measurements are relative to the reference sensor in both magnitude and phase. Thus, the unknown modal coefficients  $CF_{mn}$  and  $CB_{mn}$  will be found with relative magnitude and phase. Since the suppression is to be determined as a ratio of downstream to upstream energy, this causes no problems. Absolute pressure levels can be determined at any measurement position at any frequency from the measured transfer function if the autospectra of the reference microphone is determined in calibrated reference pressure units (as long as the signal-to-noise ratio of the reference microphone is sufficiently high).

For each measurement point,  $j$ , there is one equation in a number of unknowns that is equal to the total number of mode coefficients included in the expansion. There will be as many equations as measurement points, which puts an upper limit on the number of modes that can be discriminated. Preferably, there will be at least twice as many measurement points as unknown mode coefficients in the expansion so that spatial aliasing can be minimized.

With more measurement points than unknowns, we have an over-determined set of linear equations that must be solved for the unknown mode coefficients in the least-squares sense. In practice, there should be enough measurement points to discriminate all modes that contribute

significantly to the pressure pattern at the measurement frequency, which generally means including at least all cut-on modes.

### 3.2 Matrix Formulation

At measurement point  $j$ , we define

$$P_j = p(x_j, y_j, z_j) \quad (3-4)$$

$$X_j = (x_j, y_j, z_j) \quad (3-5)$$

$$q = (m, n) \quad (3-6)$$

$$CF_q = CF_{mn} \quad (3-7)$$

$$CB_q = CB_{mn} \quad (3-8)$$

$$\Phi_{F_{q,j}} = \cos\left(\frac{m\pi x_j}{W}\right) \cos\left(\frac{n\pi y_j}{H}\right) e^{i\kappa_q^+ z_j} \quad (3-9)$$

$$\Phi_{B_{q,j}} = \cos\left(\frac{m\pi x_j}{W}\right) \cos\left(\frac{n\pi y_j}{H}\right) e^{i\kappa_q^- z_j} \quad (3-10)$$

where  $q$  represents a numerical index that is unique for each  $(m,n)$  mode. The index  $q$  converts the two-dimensional array of mode indices into a one-dimensional array. This allows the mode number to be one of the dimensions of the set of linear equations in mode number and measurement position number. This is merely a computational convenience, and to convert from the single index,  $q$  to the double index mode designation,  $(m,n)$  is simply a matter of bookkeeping.

Using index  $q$ , we can write the pressure measurement modal expansion as

$$P_j = \sum_q [CF_q \Phi_{F_{q,j}} + CB_q \Phi_{B_{q,j}}] \quad (3-11)$$

for measurement point  $j$ . The equations for the measurements at all points can be stacked into the matrix form

$$\{P\} = [\Phi F]\{CF\} + [\Phi B]\{CB\} \quad (3-12)$$

where the square brackets denote an NPTS rows by NMODES columns matrix and the curly brackets denote an NPTS-order vector for  $\{P\}$  and an NMODES-order vector for  $\{CF\}$  and  $\{CB\}$ , where

NPTS = the number of measurement points

NMODES = the total number of modes in the expansion

The matrix formulation of the pressure measurement modal expansions will be the starting point for the development of the least squares best fit method for determining the modal coefficients, which are contained in the {CF} and {CB} vectors.

The matrix equation can be written in a simpler form by stacking the forward and backward blocks into a single matrix and vector, as follows:

$$\{P\} = [\Phi_F \quad \Phi_B] \begin{Bmatrix} CF \\ CB \end{Bmatrix} = [\Phi] \{C\} \quad (3-13)$$

where  $[\Phi]$  is an NPTS by  $2 \cdot \text{NMODES}$  matrix and  $\{C\}$  is a  $2 \cdot \text{NMODES}$  vector.

### 3.3 Mode Coefficients by Least Squares Fit and Singular Value Decomposition

There are several methods by which the mode coefficients could be found. Since the x and y modes are orthogonal, even with mean flow (in the hardwall duct), a Fourier-type expansion could be used, based on a numerical integration approximation over the measurement points.

The method chosen is based on the theory of least squares best fit of a set of data points (the pressure measurements) to a linear combination of a set of basis functions (the duct modes)<sup>3</sup>. The parameters that will be chosen (the mode coefficients) are those that minimize the  $\chi^2$  statistic, which is a measure of the difference between the measured data and the analytical fit, given by

$$\chi^2 = \sum_{j=1}^{\text{NPTS}} \left[ \frac{P_j - \sum_{i=1}^{\text{NMODES}} C_i \Phi_i(X_j)}{\sigma_j} \right]^2 \quad (3-14)$$

In the expression for  $\chi^2$ ,  $\sigma_j$  is the standard deviation associated with the measurement at point j.

The measurement standard deviation  $\sigma_j$  may or may not be known. If it is not known, it can arbitrarily be set to 1.0 at each measurement point. The ability to include the standard deviation does indicate a fundamental assumption regarding the method, however, and that is that the measurement errors follow a Gaussian (normal) random distribution about some mean value at each measurement point. This implies that there are no systematic errors in the pressure measurements.

To apply the least squares method, we first define the *design matrix*,  $[\Phi D]$  as

$$\Phi D_{ji} = \frac{\Phi_i(X_j)}{\sigma_j} \quad (3-15)$$

and define the vector  $\{PS\}$  as

$$PS_j = \frac{P_j}{\sigma_j} \quad (3-16)$$

As detailed in Press, et. al. (henceforth referred to as Numerical Recipes)<sup>4</sup>, the modal coefficient vector  $\{C\}$  is determined by solving the linear system

$$[\alpha]\{C\} = \{\beta\} \quad (3-17)$$

where

$$[\alpha] = [\Phi D]^T [\Phi D] \quad (3-18)$$

and

$$\{\beta\} = [\Phi D]^T \{PS\} \quad (3-19)$$

Although any method of solving a linear system of equations could be used to solve for  $\{C\}$  (such as Gaussian elimination), Numerical Recipes<sup>5</sup> strongly recommends the use of singular value decomposition.

Singular value decomposition (SVD) is a method of solving systems of linear equations that is particularly immune to problems caused by nearly ill-conditioned systems. If a near singularity is encountered in the system matrix, SVD will not only provide a diagnostic warning of the condition, it will attempt to eliminate the cause of the problem and give the best possible solution with the remaining information. It is the method of choice for least squares problems. The subroutines used in this program are taken directly from Numerical Recipes, and the reader is referred there for more detailed information.

In addition, the uncertainties in the modal coefficients  $C_i$  are given by the diagonal elements of the inverse of the  $[\alpha]$  matrix. That is, the variances of  $C_i$  are given by

$$\sigma^2(C_i) = Q_{ii} \quad (3-20)$$

where

$$[Q] = [\alpha]^{-1} \quad (3-21)$$

This is an estimate of the error in the modal coefficients.

To conclude this section, it is noted that the method of least squares fit and the method of Fourier expansion in modal basis functions are equivalent. This is discussed in Hamming.<sup>6</sup>

### 3.4 Acoustic Energy Flux in the Duct with Flow

The axial component of acoustic intensity flux in a hardwall rectangular duct with flow is given by

$$I_z = \text{Re} \left[ \left( 1 + M^2 \right) \rho v_z^* + \frac{M}{\rho c} p p^* + \rho c M v_z v_z^* \right] \quad (3-22)$$

where Re implies the real part of the expression, the asterisk implies taking a complex conjugate, and  $\rho$  is the ambient air density.

Substituting the modal expansions for acoustic pressure and axial velocity component and integrating over the duct cross-section (using mode orthogonality) results in the expression for energy flux in the (m,n) mode,

$$\text{FLX}_{mn} = \text{EC}_{mn} \frac{WH}{4} \quad (3-23)$$

where

$$\text{EC}_{mn} = \frac{1}{\rho c} \text{Re} \left\{ \left[ \left( 1 + M^2 \right) \frac{\frac{\kappa^*}{k}}{1 - M \frac{\kappa^*}{k}} + M + \frac{M \frac{\kappa}{k} \left( \frac{\kappa^*}{k} \right)}{\left( 1 - M \frac{\kappa}{k} \right) \left( 1 - M \frac{\kappa^*}{k} \right)} \right] C_{mn} C_{mn}^* \right\} \quad (3-24)$$

This form applies to either forward or backward traveling energy flux, depending on the choice of the propagation constant for the (m,n) mode, and for the plane at which the  $C_{mn}$  are referenced. Energy will be propagated only in cut-on modes, although there is some energy convection over short distances in the mean flow case.

To obtain the total power level (PWL) in forward travelling modes at a measurement plane upstream of the treatment and a measurement plane downstream of the treatment, the energy is found as a sum over modes:

$$E_{\text{up}}^{\text{fwd}} = \sum_{m,n} \text{FLX}_{mn}^{\text{fwd}}(\text{upstream}) \quad (3-25)$$

$$E_{\text{down}}^{\text{fwd}} = \sum_{m,n} \text{FLX}_{mn}^{\text{fwd}}(\text{downstream}) \quad (3-26)$$

The suppression of forward-travelling PWL, denoted  $\Delta\text{PWL}$ , in dB, is then given by

$$\Delta\text{PWL} = 10 \log_{10} \left( \frac{E_{\text{down}}^{\text{fwd}}}{E_{\text{up}}^{\text{fwd}}} \right) \quad (3-27)$$

This represents the measured suppression of a treatment panel located between the upstream and downstream measurement planes.

A users' guide for operation of the program RD2PMM to perform the modal measurement data analysis is included in Appendix A.

### 3.5 References for Section 3

- 
1. Motsinger, R. E., Kraft, R. E., Zwick, J. W., Vukelich, S. I., Minner, G. L., and Baumeister, K. J., "Optimization of Suppression for Two-Element Treatment Liners for Turbomachinery Exhaust Ducts", NASA CR-134997, April, 1976.
  2. Motsinger, R. E., Kraft, R. E., and Zwick, J. W., "Design of Optimum Acoustic Treatment for Rectangular Ducts with Flow", ASME 76-GT-113, March, 1976.
  3. Press, W. H., Teukolsky, S. A., Vetterling, W. T., and Flannery, B P., *Numerical Recipes in FORTRAN: The Art of Scientific Computing*, Cambridge University Press, Second Edition, 1992, pp. 665-666.
  4. Press, W. H., Teukolsky, S. A., Vetterling, W. T., and Flannery, B P., *Numerical Recipes in FORTRAN: The Art of Scientific Computing*, Cambridge University Press, Second Edition, 1992, pp. 666-667.
  5. Press, W. H., Teukolsky, S. A., Vetterling, W. T., and Flannery, B P., *Numerical Recipes in FORTRAN: The Art of Scientific Computing*, Cambridge University Press, Second Edition, 1992, pp. 670-675.
  6. Hamming, R. W., *Numerical Methods for Scientists and Engineers*, Dover Publications, 1973, Ch. 26.

#### 4. Acoustic Modal Measurement

Acoustic transmission loss and insertion loss measurements were made using a series of treatment panels in the Flow Duct Facility in the GEAE Acoustic Laboratory. Treatment panels on which testing was performed are listed in Table (4-1).

**Table 1 Treatment Panels Used for Duct Testing**

<b>Panel Number</b>	<b>Treatment Description</b>
1.1.1	Full Scale 10% Perforate SDOF
1.2.1	Half Scale 10% Perforate SDOF
2.1	Full Scale 12% Perforate SDOF
2.3	Half Scale 12% Perforate SDOF
2.5	Fifth Scale 12% Perforate SDOF
3.1	Full Scale 8% Perforate SDOF
3.3	Half Scale 8% Perforate SDOF
3.5	Fifth Scale 8% Perforate SDOF
4.1	Full Scale 90 Rayl Linear SDOF
4.2	Fifth Scale 90 Rayl Linear SDOF
5.1	Full Scale 60 Rayl Linear SDOF
6.1.1	Full Scale DDOF
6.2.1	Fifth Scale DDOF

For the transmission loss measurements, acoustic data were acquired at two planes upstream and two planes downstream of the treatment test section, with 10 microphones at each plane. The microphones in this configuration were used for the modal decomposition data analysis, and the modal energy in the forward-traveling modes upstream was compared to the energy in the forward-traveling modes downstream to determine the transmission loss.

For the insertion loss measurements, a subset of the 20 microphone positions upstream and 20 positions downstream was used to obtain an estimate of the energy flux. The time-averaged pressure-squared signals from 8 selected microphones upstream and 8 microphones downstream were summed to provide an estimation of energy flux. The transmission loss is determined by taking 10 log of the ratio of downstream  $p^2$  to upstream  $p^2$ . The transmission loss measurement was then corrected by subtracting the transmission loss for an untreated (hardwall) duct, giving the insertion loss. The insertion loss was computed very quickly on-line, so that it was available with little extra effort, whereas the modal measurement required data reduction and post-processing of the microphone data.

The measurements were made using discrete frequency excitation to a bank of loudspeakers. The discrete frequencies were chosen to be specified 1/3 octave band center frequencies. Signal enhancement techniques were used to improve signal-to-noise ratio. This involved synchronized time-domain averaging before the FFT application. Fifty (50) time

averages were used at Mach 0.0 and 500 averages were used at Mach 0.8. This approach was extremely effective in improving signal-to-noise-ratio.

Four Altec-Lansing 299-8A Speakers (50 Watts each) with a frequency range 500 to 15000 Hz. were used as the discrete sound source. The speakers were driven by JBL Model 6260 Power Amplifiers (150 Watt each channel). A Hewlett-Packard 8904A Multifunction Synthesizer was used for signal generation. The microphone arrays used Kulite transducers, Model XCS-190, rated at 5psig.

The signal conditioning amplifiers were VISHAY Model # 2310. Microphone signals were recorded on two METRUM RSR 512 Digital Tape Recorders. Each recorder had 24 tracks, of which 20 were used for upstream transducers (recorded on Metrum #1) and the 20 downstream transducer signals were recorded on Metrum # 2. Tape recorders were synchronized by means of event markers. Recorded data analyzed in post-test processing to provide input to the modal decomposition data analysis.

All transducers were calibrated for pressure amplitude at 500 Hz. Upstream transducers were calibrated for amplitude and phase relative to transducer #1 of that array. Similarly, the downstream transducers were calibrated relative the #1 transducer of that array. The #1 upstream and downstream transducers were used to obtain upstream-to-downstream magnitude and phase calibration.

Boundary Layer profiles were measured by a total pressure (impact) probe using a ROTADATA Actuator Type RTA290. The ROTADATA controller was operated under software control by an HP9133 computer via IEEE488 interface.

Validyne pressure transducers were used for measuring steady pressures. These measurements were required in the DC Flow Apparatus and for the total and static pressures used in the boundary layer profile measurements. The signals from these transducers were acquired through a 16 channel A to D converter system in the HP9133 computer. These transducers were calibrated with the help of a Druck DP1601 Digital Pressure Indicator.

Appendix B is the laboratory procedure for calibration of the acoustic data acquisition system. Appendix C gives the laboratory procedure for the reduction of the acoustic data recorded during flow duct testing.

Insertion loss data show significant repeatability scatter. It was later shown analytically that the axial variation of the sum of pressure-squared can be quite large at discrete frequencies when a limited number of propagating modes are present due to the interference of forward propagating modes alone. The errors generated by axial mode interference are sufficiently large to make the validity of the pressure-squared insertion loss as a measure of treatment effectiveness questionable. For this reason, no insertion loss data is included in this report.

The results of the modal measurement transmission loss testing are examined in the next section.

## 5. Correlation of Theory with Experiment

### 5.1 Introduction

In order to design optimum acoustic treatment, it is necessary to develop a robust acoustic prediction code and an experimental method to estimate and optimize the acoustic performance. Ultimately, the code has to be correlated with the experimental algorithm and measurement results.

In this section, in-duct attenuation predictions are compared with measured flow duct data. The flow duct test algorithm and data were introduced in Sections 3 and 4. The FORTRAN program RD2PMM was used to measure the forward and backward mode coefficients (mode amplitudes) at the upstream plane and the downstream plane as well as the attenuation of acoustic energy.

In the following sections, analytical results based on the theory discussed in Section 2 will be compared with the experimental data in Section 4. Three flow duct conditions were considered in this analysis.

**Condition 1: Hardwall Case - No Mean Flow:** Analysis of the acoustic mode phase angle shift between the downstream and upstream propagating waves in a hardwall duct without taking account of grazing flow effects.

**Condition 2: Softwall Case - No Mean Flow:** Analysis of the attenuation of the acoustic energy for the propagating modes in a softwall duct without taking account of grazing flow effects.

**Condition 3: Softwall Case - Uniform Mean Flow:** Analysis of the attenuation of the acoustic energy of the propagating modes in a softwall duct with grazing flow effects.

Because many modes are generated in the upstream region, in this section, the “cut-off” modes will be excluded in this correlation analysis and only the “cut-on” modes will be studied. These cut-off modes could be significantly attenuated in a hardwall duct within a short propagating distance. The cut-off ratio, which was first introduced by E. Rice<sup>1</sup>, is defined as:

$$\zeta^2 = \frac{1}{(k_x^2 + k_y^2)(1 - M^2)} \quad (5-1)$$

where,

---

<sup>1</sup> Rice, E. J., “Acoustic Liner Optimum Impedance for Spinning Modes with Cut-Off Ratio as the Design Criterion”, NASA TM X-73411, July, 1976.

$$k_x = \frac{m\pi}{W} \quad \text{and} \quad k_y = \frac{n\pi}{H} \quad (5-2)$$

When Equation (5-1) is used in Equation (3-2), it is seen that at  $\zeta = 1$  the radical in Equation (3-2) vanishes and this will be termed cut-off. For  $\zeta < 1$ , the axial coefficient propagation  $k_{mn}$  will be complex and damping occurs in the pressure term of Equation (3-1). Therefore, in a hardwall duct, modes with  $\zeta < 1$  are categorized as “cut-off” modes;  $\zeta > 1$  are “cut-on” modes.

## 5.2 Hardwall Case - No Mean Flow

In order to achieve good correlation between analytical predictions and experimental data, it is necessary to provide accurate physical parameters which are required for the prediction program. These parameters include: in-duct Mach number, duct geometry, boundary layer thickness, in-duct temperature, acoustic modal content, and liner impedance with grazing flow. Among these parameters, the modal content is especially critical for noise attenuation predictions.

In this section, the upstream modal content ( $z = 0''$ ) estimated in Section 4.3.1 will be used to predict the downstream modal content ( $z = 56''$ ). Then the experimentally estimated downstream modal content, shown in the Section 4.3.1, will be compared with the prediction results.

In the analytical prediction method, a translation factor was applied to the upstream mode coefficients (amplitudes and phases) to estimate the modal contents at downstream plane:

$$CF_{mn}^{\text{down}} = CF_{mn}^{\text{up}} e^{-iK\eta d} \quad (5-3)$$

where

$$k_z = K\eta$$

$$\eta : \text{normalized frequency } \frac{2\pi f H}{c}$$

H: duct height (treatment to hardwall = 4 inch)

d: acoustic wave propagation distance normalized by H

$CF_{mn}^{\text{down}}$  : mode coefficient for (m, n) mode at downstream plane

$CF_{mn}^{\text{up}}$  : mode coefficient for (m, n) mode at upstream plane

Substituting the eigenvalues ( $k_x$  and  $k_y$ ) and normalized frequencies ( $\eta$ ) into Equation (3-2) for the in-duct temperature at 526.09° R, the propagation coefficients (K) for each cut-on mode are determined and tabulated in Table (5-1).

**Table (5-1). Mode Propagation Parameters**

Frq. (Hz)	$\eta$	Mode	$k_x^*$	$k_y^*$	K
1245	2.3187	(1,1)	0.0000	0.0000	1.0000
1599	2.9779	(1,1)	0.0000	0.0000	1.0000
1599	2.9779	(2,1)	2.5133	0.0000	0.5364
2002	3.7285	(1,1)	0.0000	0.0000	1.0000
2002	3.7285	(1,2)	0.0000	3.1416	0.5386
2002	3.7285	(2,1)	2.5133	0.0000	0.7387
2502	4.6597	(1,1)	0.0000	0.0000	1.0000
2502	4.6597	(1,2)	0.0000	3.1416	0.7385
2502	4.6597	(2,1)	2.5133	0.0000	0.8421
2502	4.6597	(2,2)	2.5133	3.1416	0.5045
3149	5.8646	(1,1)	0.0000	0.0000	1.0000
3149	5.8646	(1,2)	0.0000	3.1416	0.8444
3149	5.8646	(2,1)	2.5133	0.0000	0.9035
3149	5.8646	(2,2)	2.5133	3.1416	0.7276
3149	5.8646	(3,1)	5.0265	0.0000	0.5152

\*:  $k_x$  and  $k_y$  are the eigenvalues in the x and y directions

After applying the translation factor (Equation 5-3) to the measured upstream mode coefficients (amplitudes and phases), shown in Section 5.1, the down stream mode coefficients are determined and tabulated in Table (5-2) below:

**Table (5-2). Downstream Mode Coefficients**

Frq. (Hz)	Mode	Measured Upstream		Measured Downstream		Predicted Downstream	
		p1	ph1	p2	ph2	p2	ph2
1245	1,1	0.9935	3.95	0.936	55.73	0.9935	-55.94
1599	1,1	0.7562	-66.45	0.7325	142.48	0.7562	64.82
1599	2,1	0.8232	-124.89	0.6686	51.24	0.8232	33.79
2002	1,1	0.3657	5.43	0.3372	87.25	0.3657	-105.34
2002	1,2	0.7857	-167.83	0.6866	-43.04	0.7857	21.34
2002	2,1	0.1397	94.32	0.1445	110.72	0.1397	45.04
2502	1,1	0.3597	-75.8	0.3217	27.35	0.3597	146.48
2502	1,2	0.8522	-175.37	0.7266	22.74	0.8522	-55.67
2502	2,1	0.007	-144.77	0.005	171.87	0.007	-52.30
2502	2,2	0.0809	119.15	0.0848	146.47	0.0809	33.47
3149	1,1	0.9261	-157.02	0.7499	-173.03	0.9261	178.72
3149	1,2	2.1065	170.1	1.7402	136.31	2.1065	157.82
3149	2,1	0.2149	-94.02	0.1873	133.65	0.2149	-24.32
3149	2,2	0.5545	-160.52	0.5395	-27.22	0.5545	16.66
3149	3,1	0.1483	89.1	0.2494	-38.48	0.1483	-174.54

Based on the theoretical assumption shown in Section 2.3, the predicted modal amplitude would remain unchanged in a hardwall duct while the “cut-on” acoustic wave propagates downstream. The modal phase would be shifted according to the translation factor as a function of propagation distance.

The percentage differences between the measured and predicted downstream mode coefficients are tabulated in Table (5-3) below.

**Table (5-3). Differences Between Measured and Predicted Downstream Mode Coefficients**

Frq. (Hz)	Mode	$\% = \frac{\text{Measured} - \text{Predicted}}{\text{Measured}}$	
		Amplitude	Phase
1245	1,1	-6.14%	200.38%
1599	1,1	-3.24%	54.51%
1599	2,1	-23.12%	34.06%
2002	1,1	-8.45%	220.73%
2002	1,2	-14.43%	149.58%
2002	2,1	3.32%	59.32%
2502	1,1	-11.81%	-435.58%
2502	1,2	-17.29%	344.81%
2502	2,1	-40.00%	130.43%
2502	2,2	4.60%	77.15%
3149	1,1	-23.50%	203.29%
3149	1,2	-21.05%	-15.78%
3149	2,1	-14.74%	118.20%
3149	2,2	-2.78%	161.20%
3149	3,1	40.54%	-353.59%

The above table indicates *that the measured and predicted mode coefficients do not correlate well*. This can indicate the presence of significant errors in the noise attenuation calculation.

### 5.3 Softwall Case - No Mean Flow

The acoustic panel selected for this analysis is a Single Degree Of Freedom (SDOF) Linear acoustic liner (Panel 4.1). The liner configuration is described in Table (5-4) below:

**Table (5-4). Liner Configuration for Modal Measurement Test**

DynaRohr		Panel		4.1	
Face	R3 Rayls	Diameter	Thickness	POA	NLF
Sheet	84.53	0.050"	0.025"	32%	1.49
Core & Back Skin	Core Height	Core	Type	Back	Skin
	1.0"	3/8 cell, .003" Al foil, 4.2 lb/ft <sup>3</sup>		0.032";	Aluminum

**5.3.1 Impedance Analysis**

The single frequency excitation method is used to calculate the normal incidence impedance of the test panel. The theory used in this analysis is described in Volumes 2 and 3. The in-duct temperature and pressure used are 531° R and 14.70 psi. The in-duct sound pressures are calculated based on the average of the sound pressure measured at the upstream and downstream locations and are listed in Table (5-5) below:

**Table (5-5). Data Used to Determine Duct SPL**

Frequency (Hz)	Average SPL (dB)
1250	128.85
1600	125.36
2000	133.84
2500	135.62
3150	120.07
4000	124.15

The predicted impedance levels are summarized in Table (5-6) below:

**Table (5-6). Predicted Liner Impedance Values**

Frequency (Hz)	Resistance	Reactance
1250	1.602	-1.351
1600	1.596	-0.866
2000	1.638	-0.469
2500	1.655	-0.086
3150	1.591	0.330
4000	1.599	0.849

**5.3.2 Noise Attenuation Analysis**

The acoustic treatment starts at  $z = 24.5$  and ends at  $z = 36.5$ ". Therefore, the modal amplitudes at the  $z = 24.5$  inch plane are first estimated by using Equation (5-3) with the mode coefficients measured at  $z = 0$  inch as an initial value. The axial propagation coefficients tabulated in Table (5-7) below are used in Equation (5-3):

**Table (5-7). Modal Axial Propagation Constants at Different Frequencies**

Frq. (Hz)	$\eta$	Mode	$k_x^*$	$k_y^*$	K
1250	2.3172	(1,1)	0.0000	0.0000	1.0000
1600	2.9660	(1,1)	0.0000	0.0000	1.0000
1600	2.9660	(2,1)	2.5133	0.0000	0.5310
2000	3.7075	(1,1)	0.0000	0.0000	1.0000
2000	3.7075	(1,2)	0.0000	3.1416	0.5310
2000	3.7075	(2,1)	2.5133	0.0000	0.7352
2500	4.6344	(1,1)	0.0000	0.0000	1.0000
2500	4.6344	(1,2)	0.0000	3.1416	0.7352
2500	4.6344	(2,1)	2.5133	0.0000	0.8402
2500	4.6344	(2,2)	2.5133	3.1416	0.4963
3150	5.8393	(1,1)	0.0000	0.0000	1.0000
3150	5.8393	(1,2)	0.0000	3.1416	0.8429
3150	5.8393	(2,1)	2.5133	0.0000	0.9026
3150	5.8393	(2,2)	2.5133	3.1416	0.7248
3150	5.8393	(3,1)	5.0265	0.0000	0.5089
4000	7.4150	(1,1)	0.0000	0.0000	1.0000
4000	7.4150	(1,2)	0.0000	3.1416	0.9058
4000	7.4150	(1,3)	0.0000	6.2832	0.5310
4000	7.4150	(2,1)	2.5133	0.0000	0.9408
4000	7.4150	(2,2)	2.5133	3.1416	0.8400
4000	7.4150	(2,3)	2.5133	6.2832	0.4088
4000	7.4150	(3,1)	5.0265	0.0000	0.7352
4000	7.4150	(3,2)	5.0265	3.1416	0.6008

The mode coefficients ( $p_2$  and  $ph_2$ ) at  $z = 24.5''$ , which will be used to define the noise source at the beginning of the acoustic treatment, are summarized in Table (5-8) below:

**Table (5-8). Source Mode Coefficients**

Frq. (Hz)	Mode	Measured	Upstream	Measured	Downstream
		p1	ph1	p2	ph2
1250	1,1	0.9720	-1.44	0.936	55.73
1600	1,1	1.5606	-29.31	0.7325	142.48
1600	2,1	0.9605	-60.09	0.6686	51.24
2000	1,1	0.3673	36.19	0.3372	87.25
2000	1,2	0.8138	176.31	0.6866	-43.04
2000	2,1	0.0506	103.57	0.8138	176.31
2500	1,1	0.3154	-63.98	0.3217	27.35
2500	1,2	0.9495	-161.30	0.7266	22.74
2500	2,1	0.0213	172.75	0.005	171.87
2500	2,2	0.0717	-97.38	0.0848	146.47
3150	1,1	0.7764	-147.11	0.7499	-173.03
3150	1,2	2.1600	-179.14	1.7402	136.31
3150	2,1	0.1071	-137.87	0.1873	133.65
3150	2,2	0.1831	148.70	0.5395	-27.22
3150	3,1	0.1564	156.16	0.2494	-38.48
4000	1,1	0.4526	53.34	0.4526	28.85
4000	1,2	1.0729	68.08	1.0729	-128.98
4000	1,3	1.7712	13.89	1.7712	63.28
4000	2,1	0.0759	114.64	0.0759	174.28
4000	2,2	0.2778	114.90	0.2778	86.72
4000	2,3	0.4469	-52.38	0.4469	50.42
4000	3,1	0.2278	-159.44	0.2278	83.53
4000	3,2	0.0436	120.22	0.0436	10.20

The impedance levels of the SDOF linear liner computed in Section 5.2.1 are used to define the boundary conditions along the wall from  $z = 24.5''$  to  $z = 36.5''$ . Two analytical algorithms are used to evaluate the in-duct noise attenuation:

Segment noise propagation - both transmitted and reflected acoustic waves are considered in the analysis,

Continuous noise propagation - only transmitted waves are considered.

The incident acoustic energy at the  $z = 24.5''$  plane and the transmitted acoustic energy at the  $z = 36.5''$  plane were computed for each transverse mode (x-direction) at

each frequency by a Rohr developed In-Duct Noise Propagation code. The noise attenuation at each frequency was calculated by taking the difference between the summation of the incident acoustic energy and the summation of the transmitted acoustic energy of all the cut-on transverse modes. The combined predicted attenuations are tabulated in Table (5-9):

**Table (5-9). Panel 4.1 In-duct Noise Attenuation Data (dB) at 0.0 Mach Number**

Frequency (Hz)	GEAE Test Data	Segment Algorithm	Continuous Algorithm
1250	6.4	6.92	6.93
1600	8.13	9.46	9.52
2000	7.58	9.24	13.42
2500	8.55	5.33	10.71
3150	11.51	4.09	7.58
4000	11.83	5.72	7.66

They are also illustrated in Figure (5-1):

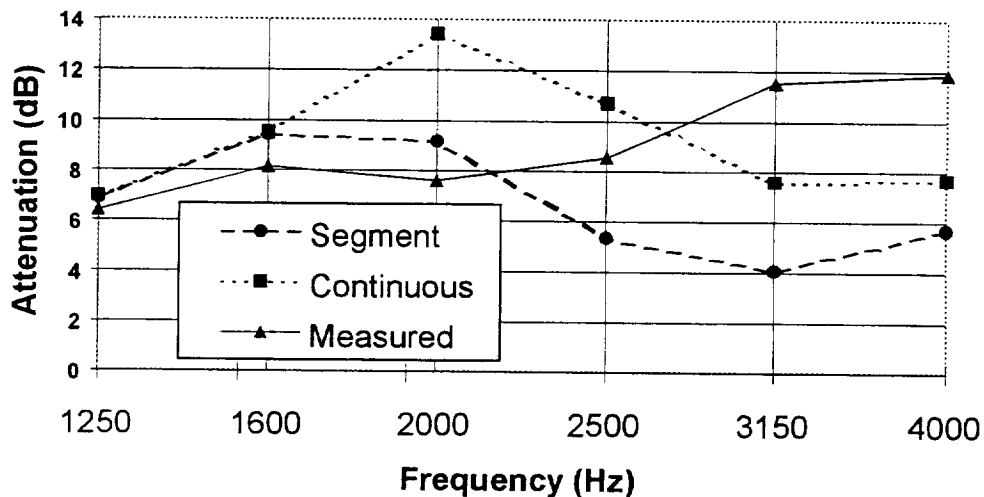


**Figure (5-1). In-Duct Noise Attenuation at Mach No. 0.0 Panel No. 4.1**

## 5.4 Softwall Case - Uniform Mean Flow

### 5.4.1 Grazing Flow Impedance Analysis

The single frequency excitation method is used to calculate the grazing flow impedance. The theory used in this analysis is described in Volumes 2 and 3. The in-duct aerodynamic parameters are listed in Table (5-10) below:

**Table (5-10). Aerodynamic Parameters for Impedance Prediction**

Static Temperature (° R)	Static Pressure (psi)	Mach Number	Displacement Boundary Layer Thickness (inch)
525.07	14.131	0.30	0.054

The in-duct sound pressures are calculated based on average Sound Pressure Levels (SPL) measured at the upstream and downstream locations, summarized in Table (5-11) below:

**Table (5-11). In-Duct Measure Sound Pressure Levels**

Frequency (Hz)	Average SPL (dB)
1250	124.97
1600	148.45
2000	135.56
2500	132.43
3150	127.18
4000	124.98

The predicted impedance levels are given in Table (5-12):

**Table (5-12). Predicted Impedances for Test Liner**

Frequency (Hz)	Resistance	Reactance
1250	1.633	-1.360
1600	1.900	-0.882
2000	1.693	-0.490
2500	1.673	-0.115
3150	1.649	0.293
4000	1.641	0.804

#### 5.4.2 Noise Attenuation Analysis

For the noise attenuation analysis in the presence of grazing flow, the axial propagation coefficients were first calculated and applied to Equation (5-3) to determine the mode coefficients at  $z = 24.5''$ . The eigenvalues in the x and y directions as well as propagation coefficients are summarized in Table (5-13) below:

**Table (5-13). Eigenvalues and Propagation Constants for Modal Computation**

Frq. (Hz)	$\eta$	Mode	$k_x^*$	$k_y^*$	K
1250	2.3302	(1,1)	0.0000	0.0000	0.7692
1600	2.9827	(1,1)	0.0000	0.0000	0.7692
1600	2.9827	(2,1)	2.5133	0.0000	0.3241
2000	3.7284	(1,1)	0.0000	0.0000	0.7692
2000	3.7284	(1,2)	0.0000	3.1416	0.3241
2000	3.7284	(2,1)	2.5133	0.0000	0.5119
2500	4.6605	(1,1)	0.0000	0.0000	0.7692
2500	4.6605	(1,2)	0.0000	3.1416	0.5119
2500	4.6605	(2,1)	2.5133	0.0000	0.6127
2500	4.6605	(2,2)	2.5133	3.1416	0.2938
3150	5.8722	(1,1)	0.0000	0.0000	0.7692
3150	5.8722	(1,2)	0.0000	3.1416	0.6153
3150	5.8722	(2,1)	2.5133	0.0000	0.6735
3150	5.8722	(2,2)	2.5133	3.1416	0.5020
3150	5.8722	(3,1)	5.0265	0.0000	0.3047
3150	5.8722	(3,2)	5.0265	0.0000	-0.0333

\*:  $k_x$  and  $k_y$  are the eigenvalues in the x and y directions

The mode coefficients at  $z = 24.5''$  are summarized in Table (5-14) below:

**Table (5-14). Mode Coefficients at Measurement Planes**

Frq. (Hz)	Mode	Measured p1	Upstream ph1	Measured p2	Downstream ph2
1250	1,1	1.3361	4.7	1.3361	95.7
1600	1,1	0.04404	57.0	0.04404	-28.1
1600	2,1	0.01514	-105.1	0.01514	-84.35
2000	1,1	0.1616	-147.7	0.1616	-74.1
2000	1,2	0.1988	-169.1	0.1988	126.8
2000	2,1	0.0206	-62.6	0.0206	-12.4
2500	1,1	0.3473	-86.7	0.3473	95.3
2500	1,2	0.8029	-166.2	0.8029	76.6
2500	2,1	0.0181	173.7	0.0181	-108.0
2500	2,2	0.2064	20.6	0.2064	-99.92
3150	1,1	0.2268	121.8	0.2268	-23.3
3150	1,2	0.5632	111.8	0.5632	-76.2
3150	2,1	0.0374	87.3	0.0374	139.4
3150	2,2	0.0909	36.9	0.0909	82.4
3150	3,1	0.1315	63.7	0.1315	155.8
3150	3,2	0.7160	-169.7	0.7160	-101.1

The mode coefficients (p2 and ph2) tabulated in the above table are used to define the noise source at the  $z = 24.5''$  plane. The grazing flow impedance levels of the SDOF linear liner computed in Section 5.3.1 are used to define the boundary conditions along the wall from  $z = 24.5''$  to  $z = 36.5''$ . The two analytical algorithms with the uniform (plug)

flow assumption, described in Section 5.2.2, are used to calculate the in-duct noise attenuation.

The incident acoustic energy at the  $z = 24.5''$  plane and the transmitted acoustic energy at the  $z = 36.5''$  plane were computed for each transverse mode (x-direction) at each frequency using the In-Duct Noise Propagation code. The noise attenuation at each frequency was calculated by taking the difference between the summation of the incident acoustic energy at  $z=24.5''$  and the summation of the transmitted acoustic energy at  $z=36.5''$  for all of the cut-on transverse modes. The combined predicted attenuations are tabulated in Table (5-15):

**Table (5-15). Panel 4.1 In-duct Noise Attenuation Data (dB)At 0.3 Mach Number**

Frequency (Hz)	GEAE Test Data	Segment Algorithm	Continuous Algorithm
1250	4.0	3.3	3.3
1600	1.8	4.1	4.1
2000	9.6	4.0	4.7
2500	5.9	4.5	7.7
3150	9.9	3.8	6.8

They are also illustrated in Figure (5-2), below:

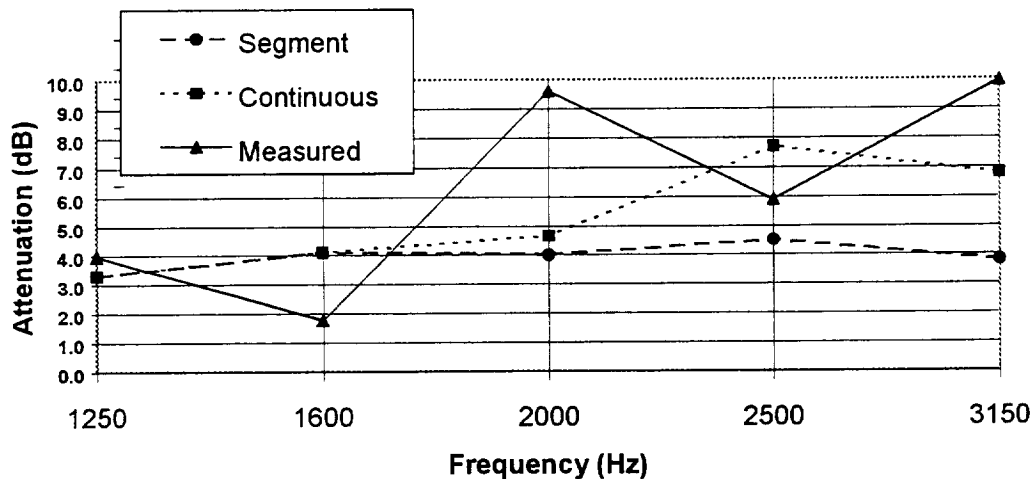


**Figure (5-2). In-Duct Noise Attenuation at Mach No. 0.3 Panel No. 4.1**

## 6. Conclusions and Recommendations

Computer programs have been written to accomplish the modal decomposition of pressure measurements made in a hardwall section of a rectangular duct. The program, although tailored to the particular output format of the tests run in the GEAE Acoustics Laboratory, is general in nature and could be adapted to other modal measurement test facilities with arbitrary sensor array placement. The program contains unique features such as the use of singular value decomposition to achieve the least squares best fit of the mode coefficients to the measured data and the ability to specify standard deviations for individual sensors in the measurement.

One obvious and relatively simple upgrade to the program would be to allow a different number of sensors at the upstream and downstream measurement planes. A version of the program could be written to use specifically chosen modes in the expansion such that the set may include some cut-off modes but the set may not form a rectangular block of indices. The program can be used with modal measurement "simulator" programs to determine optimum placement of sensor arrays for future modal measurements.

Modal measurement data taken at GEAE were transferred to Rohr, Inc, for analytical evaluation. Using a modal analysis duct propagation prediction program, Rohr compared the measured and predicted mode content. Generally, the results indicate an unsatisfactory agreement between measurement and prediction, even for full scale. This is felt to be attributable to difficulties encountered in obtaining sufficiently accurate test results, even with extraordinary care in calibrating the instrumentation and performing the test. Test difficulties precluded the ability to make measurements at frequencies high enough to be representative of sub-scale liners.

It is concluded that transmission loss measurements without ducts and data acquisition facilities specifically designed to operate with the precision and complexity required for high sub-scale frequency ranges are inadequate for evaluation of sub-scale treatment effects. If this approach is to be pursued further, it will be necessary to develop adequate sub-scale laboratory test facilities and provide instrumentation of sufficient precision and complexity.

The advantage offered by a transmission loss duct test is that it allows correlation of the scaled liner impedance with predicted liner performance under a controlled and idealized set of conditions, but under flow and sound pressure level conditions that simulate the engine duct environment. The issue becomes whether the added expense of developing a duct test facility aimed specifically at scaled treatment is cost effective considering the cost saving gained by being able to design treatment using scale model fan vehicles compared to the cost of full scale engine treatment testing. Further investigation is needed to assess the relative costs.

## 7. Appendix A - RD2PMM Program User's Guide

### 7.1 Program Versions and Choice of Number of Modes in the Expansion

The RD2PMM program calculates the modal decomposition of an array of acoustic pressure measurements taken at arbitrary positions in a hardwall segment of rectangular duct. It is important that the duct be hardwall and uniform over the full extent of the upstream or downstream modal decompositions (which are done independently), because the analysis depends upon the assumption that the axial propagation over the axial extent of the array is accurately represented by modal propagation in a uniform hardwall duct.

If the duct geometry, flow field, or wall impedance varies from uniform over the measurement segment, this assumption is violated. It is further assumed that the slug flow (infinitely thin boundary layer) assumption is an accurate representation of the acoustic propagation. Under these conditions, the duct modes are orthogonal, and no energy is carried in the cross-modes.

The input parameters include:

- Case description
- Duct cross section geometry
- Duct axial geometry
- Frequency of measurement
- Duct flow Mach number
- Ambient air temperature in duct
- Number of measurement points in the sensor array
- Number of x-modes and y-modes to be used in the modal expansion
- The number of the designated reference sensor
- SPL measured at the reference sensor
- An index to specify only forward or both forward and backward modes
- The singularity factor for the singular value decomposition matrix solution
- Coordinates and complex pressure measured at each sensor
- Standard deviation of the measurement at each sensor

There are two slightly different versions of the program, RD2PMM2 and RD2PMM3 (the original version, RD2PMM1, was replaced by RD2PMM3). The programs are distinguished by the means of choosing the modes used in the modal expansion. In RD2PMM3, the modes in the expansion are specified as a rectangular block of indices, for example 3 x-modes and 2 y-modes. This 3 by 2 block, illustrated in Table (A-1) below, contains 6 modes, some of which may be cut-off.

**Table (A-1) Block of (MX,NY) modes chosen for modal expansion in RD2PMM3.**

(1,1)	(1,2)
(2,1)	(2,2)
(3,1)	(3,2)

RD2PMM3 then allows the user the option of repeating the decomposition with a different set of component modes (say 3 x-modes by 3 y-modes) for as many cases as desired.

The RD2PMM2 version automatically finds all cut-on modes at the frequency of measurement and performs the decomposition in only those modes. No cut-off modes are included in the expansion. The block index specification in the input data file is ignored in this case.

One must take some care in the choice of mode numbers for the modal expansion. The number of modes in the expansion should not exceed the number of sensors in the upstream or the downstream array (it is assumed in both current program versions that both upstream and downstream arrays have the same number of sensors, although this restriction is not formally necessary and could be relaxed.) For instance, if there are 20 sensors in each array, the maximum number of modes would be 20 (20 forward propagating or, more likely, 10 forward propagating and 10 backward propagating).

Having the same number of modes as sensors, however, is like trying to find 20 coefficients of a Fourier series from 20 data points. Spatial aliasing problems will occur, and accuracy, particularly for the higher order modes, will be degraded. It would be better to choose about half the number of modes in the expansion as measurement points. In our example, this would mean expanding in 5 forward-propagating and 5 backward-propagating modes.

Listings of the program are not included with this report since they are still subject to debugging and improvement. Current versions of the programs are available from the author for interested parties. Since it is considered to be a research code, no guarantees can be made regarding program applicability or accuracy.

## **7.2 Program Input File**

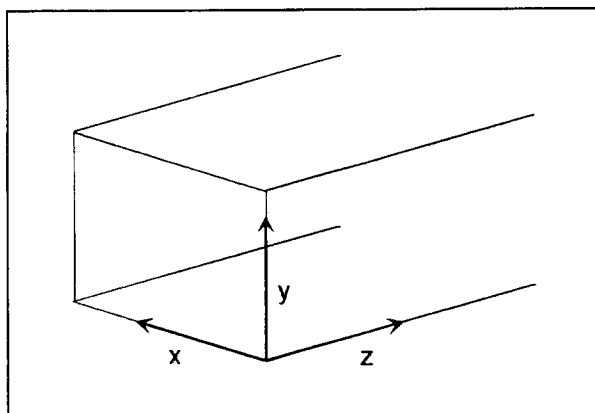
The input file for the program is an ASCII "card" file with a series of records. This file is generated as part of the modal measurement data reduction procedure, and is thus provided by the Acoustic Laboratory. The format for the input file is provided on the following page.

In order to change any options or input in the data file, any ASCII text editor may be used. For instance, it may be desired to expand only in forward-travelling modes, ignoring any contribution from backward-travelling modes, in which case a 0 would be entered in the IBKWD position.

RD2PMM2.FOR or RD2PMM3.FOR INPUT SHEET  
 Separate variables by spaces or comma  
 Records read in ASCII format

'Case Description'		Up to 60 characters					
HTIN	WDIN	Duct width (x) and height (y), inches					
DTP	DDA	Distance from Plane 1 to start of treatment and distance from Plane 1 upstream to Plane 1 downstream, inches					
FRQHZ		Frequency, Hz.					
FMACH	TDEGF	Duct Mach #, Temperature, degF					
NPTS		Number of measurement points (sensors), upstream Assumed to be same number upstream and downstream for 2-plane comparison					
NMX	NMY	Number of x-modes and y-modes to used in modal expansion					
NREF	SPLR	Reference sensor designated number, SPL at reference sensor					
IBKWD		= 0 if no backward modes assumed = 1 for both fwd and bkwd					
WFAC		SVD singularity factor (~1.E-6)					
NP	X	Y	Z	PTFR	PTFI	STD	Measured data input at each point repeat for each point
...							

NP = Designated sensor number  
 X,Y,Z = sensor coordinates, in.  
 PTFR = real part of pressure transfer function  
 PTFI = imaginary part of pressure transfer function  
 STD = sensor assumed standard deviation, usually 1.0  
 Inverse of sensor STD is weighting factor



The WFAC parameter is used in the singular value decomposition (SVD) to determine which terms are discarded. The choice of this value depends somewhat on the precision of the computer being used, but is otherwise more dependent upon the artistry of the user. If any modes generate WFAC values smaller than this amount, they will be discarded from the expansion, per the SVD procedure. A value around 1.E-6 is a reasonable guess.

The standard deviation of the measurement at each sensor (STD) is normally not known very accurately. Its determination would require a large number of repeat experiments, usually an unaffordable luxury. If the standard deviations of the measurement are unknown, set STD to 1.0 for each sensor (only relative values of STD are significant).

If one or more sensors are known to be defective, their contribution to the whole can be diminished by arbitrarily increasing STD by some factor. For instance, if STD for a given sensor is set to 2.0 (all others being 1.0), the weighting given to the offending sensor in the expansion is 1/2 or half the weighting of all the others.

### 7.3 Program Output

The following data, which will be illustrated in a sample case in the following section, is included in the output data file for both versions of the program:

- Input data
- Input and output datafile names
- Modes used in expansion
- Calculated modal propagation constants and axial wavelengths
- Mode number/index key
- SVD output parameters
- Measured mode coefficients, all planes and directions
- Mode coefficient standard deviations of the fit
- If the two-plane (upstream, downstream) option is used, the energy flux, forward and backward, upstream and downstream, and  $\Delta$ PWL is computed and printed.

The pressure mode coefficients can be directly transferred to duct propagation prediction programs such as the GE RFDP code, or the pressure can be expanded in modes over the source plane for input to FEM-type codes.

The output file is in standard ASCII format so that the results can be easily printed or imported into databases or spreadsheets for further analysis.

## 7.4 Running the Programs

For convenience, the FORTRAN executable files RD2PMM2.EXE and RD2PMM3.EXE should be copied into the subdirectory in which the input files reside and in which the output files will be written.

After starting the program, the user will be asked to enter the number of planes for computation of mode coefficients. If only one set of measurements are to be analyzed (either upstream or downstream), enter 1. If both upstream and downstream planes are to be analyzed, enter 2.

If only 1 plane is being analyzed, the program will then ask for the name of the input data file. If 2 planes of data are being analyzed the program will ask for both upstream and downstream input data file names. The program then requests the name of the output data file.

If RD2PMM2 is being run, the program will execute and stop. If RD2PMM3 is being run, the program will ask for the number of x-modes and y-modes to be included in the expansion. If another case is desired, RD2PMM3 will ask the user to enter 1, after which another mode number pair is requested. If the user enters anything other than 1 when asked if there is another case, the program will quit.

The output file is written to the current subdirectory using the filename input by the user.

## 7.5 Sample Case

A sample case taken directly from a modal measurement in the 4 inch by 5 inch duct in the GEAE Acoustics Laboratory is included here for illustration. This case is the measurement at 2500 Hz., Mach 0.0, for Test Panel 4.1, a 1 inch deep wiremesh faceplate SDOF treatment panel (the details of these tests are reported on elsewhere).

At 2500 Hz., there are four modes cut-on. These are the (1,1), (2,1), (1,2), and (2,2) modes, which just happens to be a square block of indices.

The upstream modal measurement resulted in the input data file UP410005.DAT:

---

```

P41-00-05.FRQ                Processed time:Tue Jun  6 07:11:03
4.000      5.000
24.50     56.00
 2502.441
0.000      70.000
20
 2          4
 1          139.895
 1
0.10E-05
 1  4.010  4.920  0.000  0.100000E+01  0.000000E+00  1.00
 2  4.010  3.005  0.000  0.986482E+00  0.539242E-01  1.00
 3  4.010  1.650  0.000  0.901976E+00 -0.552247E-01  1.00
 4  4.010  0.030  0.000  0.868987E+00 -0.852066E-01  1.00
 5  2.000  0.000  0.000  0.916673E-01  0.242227E+00  1.00
 6  0.000  0.045  0.000 -0.777912E+00  0.612961E+00  1.00
 7  0.000  1.655  0.000 -0.724785E+00  0.557766E+00  1.00
 8  0.000  2.920  0.000 -0.835292E+00  0.719708E+00  1.00
 9  0.000  4.905  0.000 -0.727773E+00  0.528255E+00  1.00
10  2.000  5.000  0.000  0.157300E+00  0.276621E+00  1.00
11  4.010  4.920  1.005  0.728650E+00 -0.921396E+00  1.00
12  4.010  3.005  1.005  0.667809E+00 -0.933248E+00  1.00
13  4.010  1.650  1.005  0.519296E+00 -0.948466E+00  1.00
14  4.010  0.030  1.005  0.597250E+00 -0.110330E+01  1.00
15  2.000  0.000  1.005  0.239692E+00 -0.229031E-01  1.00
16  0.000  0.045  1.005  0.436094E-01  0.898323E+00  1.00
17  0.000  1.655  1.005  0.567900E-01  0.873310E+00  1.00
18  0.000  2.920  1.005 -0.106060E+00  0.878621E+00  1.00
19  0.000  4.905  1.005 -0.998554E-01  0.817884E+00  1.00
20  2.000  5.000  1.005  0.313136E+00 -0.829904E-01  1.00

```

---

The downstream modal measurement resulted in the input data file DP410005.DAT:

---

P41-00-05.FRQ                      Processed time:Tue Jun 6 07:11:03

4.000            5.000  
24.50            56.00  
2502.441  
0.000            70.000  
20  
2                4  
1                139.895  
1

0.10E-05

1	4.010	4.945	0.000	0.372860E+00	-0.236690E+00	1.00
2	4.010	3.350	0.000	0.973588E+00	0.226096E-01	1.00
3	4.010	1.680	0.000	0.960073E+00	-0.833162E-02	1.00
4	4.010	0.070	0.000	0.970684E+00	0.409265E-01	1.00
5	2.000	0.000	0.000	0.780312E+00	-0.127245E+00	1.00
6	0.000	0.080	0.000	0.601760E+00	-0.323001E+00	1.00
7	0.000	1.675	0.000	0.505032E+00	-0.327699E+00	1.00
8	0.000	3.355	0.000	0.374523E+00	-0.278524E+00	1.00
9	0.000	4.945	0.000	0.335106E+00	-0.240291E+00	1.00
10	2.000	5.000	0.000	0.668857E+00	-0.112959E+00	1.00
11	4.010	3.945	1.010	0.725774E+00	-0.608125E+00	1.00
12	4.010	3.350	1.010	0.792234E+00	-0.605890E+00	1.00
13	4.010	1.680	1.010	0.770739E+00	-0.637691E+00	1.00
14	4.010	0.070	1.010	0.752161E+00	-0.728808E+00	1.00
15	2.000	0.000	1.010	0.280125E+00	-0.699518E+00	1.00
16	0.000	0.080	1.010	-0.229635E+00	-0.670994E+00	1.00
17	0.000	1.675	1.010	-0.267258E+00	-0.572909E+00	1.00
18	0.000	3.355	1.010	-0.277127E+00	-0.510695E+00	1.00
19	0.000	4.945	1.010	-0.291671E+00	-0.449993E+00	1.00
20	2.000	5.000	1.010	0.200445E+00	-0.527979E+00	1.00

---

The output from RD2PMM2, for the case with cut-on modes only, is the following:

PROGRAM RD2PPMM2 - INCLUDES CUT-ON MODES ONLY  
RECTANGULAR DUCT MODAL MEASUREMENT DATA ANALYSIS

CASE HEADING

\*\*\*\*\*  
P41-00-05.FRQ                      Processed time:Tue Jun 6 07:11:03  
\*\*\*\*\*

OUTPUT DATAFILE = C410005X.DAT

INPUT DATAFILE = UP410005.DAT                      AT PLANE PAIR    1

INPUT DATAFILE = DP410005.DAT                      AT PLANE PAIR    2

DUCT HEIGHT (Y) =    4.00000 in       .33333 ft  
DUCT WIDTH (X) =    5.00000 in       .41667 ft  
DIST FROM UPSTRM SENSOR PLANE TO TRTMT LEADING EDGE =   24.50000 in     2.04167 ft  
DIST FROM UPSTREAM SENSOR #1 TO DWNSTREAM SENSOR #1 =   56.00000 in     4.66667 ft

AIR TEMP =    70.00000 degF  
DUCT MACH NO. =    .00000

FREQUENCY =    2502.44100 Hz

SPEED OF SOUND =   1128.06500 ft/s  
WAVE NUMBER =    13.93830 1/ft  
SVD SINGULARITY FACTOR =  1.00000E-06

NUMBER OF MEASUREMENT POINTS =    20  
NUMBER OF X-MODES CONSIDERED =     4  
NUMBER OF Y-MODES CONSIDERED =     2

PRESSURE REFERENCE SENSOR DESIGNATION =    1  
PRESSURE REFERENCE SPL =    139.895 dB

J	DSGN	X, in.	Y, in.	Z, in.	PTFReal	PTFImag	Std Dev
1	1	4.9200	4.0100	.0000	1.0000E+00	0.0000E+00	1.000
2	2	3.0050	4.0100	.0000	9.8648E-01	-5.3924E-02	1.000
3	3	1.6500	4.0100	.0000	9.0198E-01	5.5225E-02	1.000
4	4	.0300	4.0100	.0000	8.6899E-01	8.5207E-02	1.000
5	5	.0000	2.0000	.0000	9.1667E-02	-2.4223E-01	1.000
6	6	.0450	.0000	.0000	-7.7791E-01	-6.1296E-01	1.000
7	7	1.6550	.0000	.0000	-7.2478E-01	-5.5777E-01	1.000
8	8	2.9200	.0000	.0000	-8.3529E-01	-7.1971E-01	1.000
9	9	4.9050	.0000	.0000	-7.2777E-01	-5.2825E-01	1.000
10	10	5.0000	2.0000	.0000	1.5730E-01	-2.7662E-01	1.000
11	11	4.9200	4.0100	1.0050	7.2865E-01	9.2140E-01	1.000
12	12	3.0050	4.0100	1.0050	6.6781E-01	9.3325E-01	1.000
13	13	1.6500	4.0100	1.0050	5.1930E-01	9.4847E-01	1.000
14	14	.0300	4.0100	1.0050	5.9725E-01	1.1033E+00	1.000
15	15	.0000	2.0000	1.0050	2.3969E-01	2.2903E-02	1.000
16	16	.0450	.0000	1.0050	4.3609E-02	-8.9832E-01	1.000
17	17	1.6550	.0000	1.0050	5.6790E-02	-8.7331E-01	1.000
18	18	2.9200	.0000	1.0050	-1.0606E-01	-8.7862E-01	1.000
19	19	4.9050	.0000	1.0050	-9.9855E-02	-8.1788E-01	1.000
20	20	5.0000	2.0000	1.0050	3.1314E-01	8.2990E-02	1.000

PROPAGATION CONSTANTS (1/ft - k-MULTIPLIED)  
& AXIAL WAVELENGTH, inches    F => Fwd, B => Bkwd

MX	NY	RePKF	ImPKF	ZWLF	RePKB	ImPKB	ZWLB
1	1	13.938300	.000000	5.409	-13.938300	.000000	-5.409
1	2	10.268870	.000000	7.342	-10.268870	.000000	-7.342
2	1	11.722930	.000000	6.432	-11.722930	.000000	-6.432
2	2	6.971423	.000000	10.815	-6.971423	.000000	-10.815
3	1	.000000	5.754962	*****	.000000	-5.754962	*****
3	2	.000000	11.042920	*****	.000000	-11.042920	*****
4	1	-.000001	17.814720	*****	.000001	-17.814720	*****
4	2	-.000001	20.154170	*****	.000001	-20.154170	*****

NUMBER OF CUT-ON MODES = 4  
 PROBLEM MODE ORDER = 8

MODE#	MXF	NYF	MODE#	MXB	NYB
1	1	1	5	1	1
2	2	1	6	2	1
3	1	2	7	1	2
4	2	2	8	2	2

FOR SUCCESSFUL SVD, INFO SHOULD BE ZERO. INFO = 0

J,AWSV = 1 5.299961  
 J,AWSV = 2 5.166289  
 J,AWSV = 3 4.531259  
 J,AWSV = 4 4.109190  
 J,AWSV = 5 3.490297  
 J,AWSV = 6 2.429513  
 J,AWSV = 7 2.359705  
 J,AWSV = 8 1.239705

WMAX = 5.3000E+00 WMIN = 5.3000E-06

MEASURED MODE COEFFICIENTS

FORWARD			COMPLEX COEFFICIENT		MAGNITUDE	PHASE, deg
MODE#	MX	NY				
1	1	1	1.38367E-01	-2.83424E-01	3.15396E-01	-63.9785
2	2	1	-2.11092E-02	2.68653E-03	2.12795E-02	172.7470
3	1	2	-8.99362E-01	-3.04402E-01	9.49480E-01	-161.3008
4	2	2	-9.20850E-03	-7.11376E-02	7.17312E-02	-97.3757

BACKWARD			COMPLEX COEFFICIENT		MAGNITUDE	PHASE, deg
MODE#	MX	NY				
5	1	1	-4.28227E-02	-2.34929E-03	4.28871E-02	-176.8598
6	2	1	-1.54780E-02	1.61426E-02	2.23641E-02	133.7959
7	1	2	4.48531E-02	-6.99747E-03	4.53956E-02	-8.8672
8	2	2	4.18779E-02	3.75269E-02	5.62319E-02	41.8636

MODE COEFFICIENT FIT STANDARD DEVIATIONS

J StdDev  
 1 2.4350E-01  
 2 3.2969E-01  
 3 3.3077E-01  
 4 5.9497E-01  
 5 2.4350E-01  
 6 3.2969E-01  
 7 3.3077E-01  
 8 5.9497E-01

PROGRAM RD2PPMM2 - INCLUDES CUT-ON MODES ONLY  
 RECTANGULAR DUCT MODAL MEASUREMENT DATA ANALYSIS

CASE HEADING

\*\*\*\*\*  
 P41-00-05.FRQ Processed time:Tue Jun 6 07:11:03  
 \*\*\*\*\*

OUTPUT DATAFILE = C410005X.DAT

INPUT DATAFILE = UP410005.DAT AT PLANE PAIR 1

INPUT DATAFILE = DP410005.DAT AT PLANE PAIR 2

DUCT HEIGHT (Y) = 4.00000 in .33333 ft  
 DUCT WIDTH (X) = 5.00000 in .41667 ft  
 DIST FROM UPSTRM SENSOR PLANE TO TRTMT LEADING EDGE = 24.50000 in 2.04167 ft  
 DIST FROM UPSTREAM SENSOR #1 TO DWNSTREAM SENSOR #1 = 56.00000 in 4.66667 ft

AIR TEMP = 70.00000 degF  
 DUCT MACH NO. = .00000

FREQUENCY = 2502.44100 Hz

SPEED OF SOUND = 1128.06500 ft/s  
 WAVE NUMBER = 13.93830 1/ft  
 SVD SINGULARITY FACTOR = 1.00000E-06

NUMBER OF MEASUREMENT POINTS = 20  
 NUMBER OF X-MODES CONSIDERED = 4  
 NUMBER OF Y-MODES CONSIDERED = 2

PRESSURE REFERENCE SENSOR DESIGNATION = 1  
 PRESSURE REFERENCE SPL = 139.895 dB

UPSTREAM -> DOWNSTREAM TRANSFER FUNCTION = 3.728600E-01 2.366900E-01

J	DSGN	X, in.	Y, in.	Z, in.	PTFReal	PTFImag	Std Dev
1	1	4.9450	4.0100	.0000	3.7286E-01	2.3669E-01	1.000
2	2	3.3500	4.0100	.0000	9.7359E-01	-2.2610E-02	1.000
3	3	1.6800	4.0100	.0000	9.6007E-01	8.3316E-03	1.000
4	4	.0700	4.0100	.0000	9.7068E-01	-4.0927E-02	1.000
5	5	.0000	2.0000	.0000	7.8031E-01	1.2724E-01	1.000
6	6	.0800	.0000	.0000	6.0176E-01	3.2300E-01	1.000
7	7	1.6750	.0000	.0000	5.0503E-01	3.2770E-01	1.000
8	8	3.3550	.0000	.0000	3.7452E-01	2.7852E-01	1.000
9	9	4.9450	.0000	.0000	3.3511E-01	2.4029E-01	1.000
10	10	5.0000	2.0000	.0000	6.6886E-01	1.1296E-01	1.000
11	11	3.9450	4.0100	1.0100	7.2577E-01	6.0812E-01	1.000
12	12	3.3500	4.0100	1.0100	7.9223E-01	6.0589E-01	1.000
13	13	1.6800	4.0100	1.0100	7.7074E-01	6.3769E-01	1.000
14	14	.0700	4.0100	1.0100	7.5216E-01	7.2881E-01	1.000
15	15	.0000	2.0000	1.0100	2.8012E-01	6.9952E-01	1.000
16	16	.0800	.0000	1.0100	-2.2964E-01	6.7099E-01	1.000
17	17	1.6750	.0000	1.0100	-2.6726E-01	5.7291E-01	1.000
18	18	3.3550	.0000	1.0100	-2.7713E-01	5.1069E-01	1.000
19	19	4.9450	.0000	1.0100	-2.9167E-01	4.4999E-01	1.000
20	20	5.0000	2.0000	1.0100	2.0044E-01	5.2798E-01	1.000

PROPAGATION CONSTANTS (1/ft - k-MULTIPLIED)  
 & AXIAL WAVELENGTH, inches F => Fwd, B => Bkwd

MX NY	RePKF	ImPKF	ZWLF	RePKB	ImPKB	ZWLB
1 1	13.938300	.000000	5.409	-13.938300	.000000	-5.409
1 2	10.268870	.000000	7.342	-10.268870	.000000	-7.342
2 1	11.722930	.000000	6.432	-11.722930	.000000	-6.432
2 2	6.971423	.000000	10.815	-6.971423	.000000	-10.815
3 1	.000000	5.754962	*****	.000000	-5.754962	*****
3 2	.000000	11.042920	*****	.000000	-11.042920	*****
4 1	-.000001	17.814720	*****	.000001	-17.814720	*****
4 2	-.000001	20.154170	*****	.000001	-20.154170	*****

NUMBER OF CUT-ON MODES = 4  
 PROBLEM MODE ORDER = 8

MODE#	MXF	NYF	MODE#	MXB	NYB
1	1	1	5	1	1
2	2	1	6	2	1
3	1	2	7	1	2
4	2	2	8	2	2

FOR SUCCESSFUL SVD, INFO SHOULD BE ZERO. INFO = 0

J,AWSV = 1 5.269103  
 J,AWSV = 2 5.139447  
 J,AWSV = 3 4.609812  
 J,AWSV = 4 4.187496  
 J,AWSV = 5 3.498797  
 J,AWSV = 6 2.471864  
 J,AWSV = 7 2.364881

J,AWSV = 8 1.265114  
 WMAX = 5.2691E+00 WMIN = 5.2691E-06

MEASURED MODE COEFFICIENTS

FORWARD			COMPLEX COEFFICIENT		MAGNITUDE	PHASE, deg
MODE#	MX	NY				
1	1	1	2.24280E-01	1.86984E-01	2.92001E-01	39.8182
2	2	1	2.46207E-02	2.21279E-02	3.31032E-02	41.9477
3	1	2	-1.55680E-01	5.94458E-02	1.66644E-01	159.1009
4	2	2	-9.58030E-04	3.01652E-02	3.01804E-02	91.8191

BACKWARD			COMPLEX COEFFICIENT		MAGNITUDE	PHASE, deg
MODE#	MX	NY				
5	1	1	1.10624E-02	3.32900E-02	3.50799E-02	71.6182
6	2	1	-6.15369E-03	-3.25182E-03	6.96005E-03	-152.1465
7	1	2	2.22200E-02	-6.40232E-02	6.77694E-02	-70.8601
8	2	2	2.21101E-02	-2.86427E-03	2.22949E-02	-7.3813

MODE COEFFICIENT FIT STANDARD DEVIATIONS  
 J StdDev

1	2.4263E-01
2	3.2539E-01
3	3.2883E-01
4	5.8360E-01
5	2.4263E-01
6	3.2539E-01
7	3.2883E-01
8	5.8360E-01

FORWARD ENERGY UPSTREAM = 2.4983E+00 WATTS

BACKWARD ENERGY UPSTREAM = -1.7467E-02 WATTS

FORWARD ENERGY DOWNSTREAM = 3.4903E-01 WATTS

BACKWARD ENERGY DOWNSTREAM = -1.5980E-02 WATTS

DELTA PWL = -8.5478E+00 dB

A sample output file from RD2PMM3, with just two different mode expansion cases, is the following

```

PROGRAM RD2PMM3
RECTANGULAR DUCT MODAL MEASUREMENT DATA ANALYSIS

CASE HEADING
*****
P41-00-05.FRQ          Processed time:Tue Jun  6 07:11:03
*****

OUTPUT DATAFILE = M410005X.DAT

INPUT DATAFILE = UP410005.DAT          AT PLANE PAIR  1

INPUT DATAFILE = DP410005.DAT          AT PLANE PAIR  2

DUCT HEIGHT (Y) =    4.00000 in    .33333 ft
DUCT WIDTH (X) =    5.00000 in    .41667 ft
DIST FROM UPSTRM SENSOR PLANE TO TRTMT LEADING EDGE =    24.50000 in    2.04167 ft
DIST FROM UPSTREAM SENSOR #1 TO DWNSTREAM SENSOR #1 =    56.00000 in    4.66667 ft

AIR TEMP =    70.00000 degF
DUCT MACH NO. =    .00000

FREQUENCY =    2502.44100 Hz

SPEED OF SOUND =    1128.06500 ft/s
WAVE NUMBER =    13.93830 1/ft
SVD SINGULARITY FACTOR =    1.00000E-06

PRESSURE REFERENCE SENSOR DESIGNATION =    1
PRESSURE REFERENCE SPL =    139.895 dB

   J   DSGN      X, in.      Y, in.      Z, in.      PTFReal      PTFImag      Std Dev
1     1       4.9200       4.0100       .0000       1.0000E+00       0.0000E+00       1.000
2     2       3.0050       4.0100       .0000       9.8648E-01       -5.3924E-02       1.000
3     3       1.6500       4.0100       .0000       9.0198E-01       5.5225E-02       1.000
4     4        .0300       4.0100       .0000       8.6899E-01       8.5207E-02       1.000
5     5        .0000       2.0000       .0000       9.1667E-02       -2.4223E-01       1.000
6     6        .0450        .0000       .0000       -7.7791E-01       -6.1296E-01       1.000
7     7       1.6550        .0000       .0000       -7.2478E-01       -5.5777E-01       1.000
8     8       2.9200        .0000       .0000       -8.3529E-01       -7.1971E-01       1.000
9     9       4.9050        .0000       .0000       -7.2777E-01       -5.2825E-01       1.000
10    10      5.0000       2.0000       .0000       1.5730E-01       -2.7662E-01       1.000
11    11      4.9200       4.0100       1.0050       7.2865E-01       9.2140E-01       1.000
12    12      3.0050       4.0100       1.0050       6.6781E-01       9.3325E-01       1.000
13    13      1.6500       4.0100       1.0050       5.1930E-01       9.4847E-01       1.000
14    14        .0300       4.0100       1.0050       5.9725E-01       1.1033E+00       1.000
15    15        .0000       2.0000       1.0050       2.3969E-01       2.2903E-02       1.000
16    16        .0450        .0000       1.0050       4.3609E-02       -8.9832E-01       1.000
17    17       1.6550        .0000       1.0050       5.6790E-02       -8.7331E-01       1.000
18    18       2.9200        .0000       1.0050       -1.0606E-01       -8.7862E-01       1.000
19    19       4.9050        .0000       1.0050       -9.9855E-02       -8.1788E-01       1.000
20    20       5.0000       2.0000       1.0050       3.1314E-01       8.2990E-02       1.000

NUMBER OF MEASUREMENT POINTS =    20
NUMBER OF X-MODES =    4
NUMBER OF Y-MODES =    2

PROPAGATION CONSTANTS (1/ft - k-MULTIPLIED)
& AXIAL WAVELENGTH, inches      F => Fwd, B => Bkwd
MX NY      RePKF      ImPKF      ZWLF      RePKB      ImPKB      ZWLB
1  1      13.938300      .000000      5.409      -13.938300      .000000      -5.409
1  2      10.268870      .000000      7.342      -10.268870      .000000      -7.342
2  1      11.722930      .000000      6.432      -11.722930      .000000      -6.432
2  2      6.971423      .000000      10.815      -6.971423      .000000      -10.815
3  1      .000000      5.754962      *****      .000000      -5.754962      *****
3  2      .000000      11.042920      *****      .000000      -11.042920      *****

```

```

4 1  -.000001  17.814720  *****  .000001  -17.814720  *****
4 2  -.000001  20.154170  *****  .000001  -20.154170  *****

```

```

MX  NY  FWD COL#  BKWD COL#
1   1   1         9
2   1   2        10
3   1   3        11
4   1   4        12
1   2   5        13
2   2   6        14
3   2   7        15
4   2   8        16

```

FOR SUCCESSFUL SVD, INFO SHOULD BE ZERO. INFO = 0

```

J,AWSV = 1 14.806920
J,AWSV = 2 14.010460
J,AWSV = 3 6.947521
J,AWSV = 4 6.765834
J,AWSV = 5 4.981485
J,AWSV = 6 4.476947
J,AWSV = 7 4.142041
J,AWSV = 8 3.893124
J,AWSV = 9 3.518194
J,AWSV = 10 2.802498
J,AWSV = 11 2.455015
J,AWSV = 12 2.365283
J,AWSV = 13 1.749348
J,AWSV = 14 1.697060
J,AWSV = 15 1.172557
J,AWSV = 16 1.086329

```

WMAX = 1.4807E+01 WMIN = 1.4807E-05

MEASURED MODE COEFFICIENTS

```

FORWARD
MX  NY  COMPLEX COEFFICIENT  MAGNITUDE  PHASE, deg
1   1   1.34938E-01 -2.90361E-01  3.20184E-01  -65.0744
1   2   -8.99480E-01 -3.07793E-01  9.50684E-01  -161.1095
2   1   -2.57174E-02  2.00361E-02  3.26010E-02  142.0783
2   2   -1.37300E-03 -7.16467E-02  7.16599E-02  -91.0978
3   1   6.66241E-03  4.38428E-02  4.43461E-02  81.3594
3   2   2.52635E-02  1.91754E-02  3.17165E-02  37.1991
4   1   -1.65993E-02 -4.85092E-02  5.12706E-02  -108.8904
4   2   -2.27930E-02 -2.02527E-02  3.04908E-02  -138.3773

```

```

BACKWARD
MX  NY  COMPLEX COEFFICIENT  MAGNITUDE  PHASE, deg
1   1   -4.51382E-02 -1.29154E-02  4.69496E-02  -164.0325
1   2   3.93688E-02 -7.67778E-03  4.01105E-02  -11.0354
2   1   1.59755E-03  3.13039E-02  3.13446E-02  87.0785
2   2   5.09446E-02  5.22596E-02  7.29823E-02  45.7300
3   1   5.72343E-03 -2.77855E-03  6.36223E-03  -25.8952
3   2   -8.61400E-03 -1.00824E-02  1.32611E-02  -130.5092
4   1   -5.76631E-04  2.68092E-03  2.74223E-03  102.1386
4   2   -6.83364E-03 -3.14445E-03  7.52238E-03  -155.2908

```

MODE COEFFICIENT FIT STANDARD DEVIATIONS

```

J  StdDev
1  2.6427E-01
2  4.0616E-01
3  7.3369E-01
4  4.4145E-01
5  3.3911E-01
6  6.6382E-01
7  5.3950E-01
8  4.4201E-01
9  2.6427E-01
10 4.0616E-01

```

11 4.5310E-01  
 12 9.9294E-02  
 13 3.3911E-01  
 14 6.6382E-01  
 15 2.1396E-01  
 16 8.1730E-02

PROGRAM RD2PMM3  
 RECTANGULAR DUCT MODAL MEASUREMENT DATA ANALYSIS

CASE HEADING

\*\*\*\*\*  
 P41-00-05.FRQ Processed time:Tue Jun 6 07:11:03  
 \*\*\*\*\*

OUTPUT DATAFILE = M410005X.DAT

INPUT DATAFILE = UP410005.DAT AT PLANE PAIR 1

INPUT DATAFILE = DP410005.DAT AT PLANE PAIR 2

DUCT HEIGHT (Y) = 4.00000 in .33333 ft  
 DUCT WIDTH (X) = 5.00000 in .41667 ft  
 DIST FROM UPSTRM SENSOR PLANE TO TRTMT LEADING EDGE = 24.50000 in 2.04167 ft  
 DIST FROM UPSTREAM SENSOR #1 TO DWNSTREAM SENSOR #1 = 56.00000 in 4.66667 ft

AIR TEMP = 70.00000 degF  
 DUCT MACH NO. = .00000

FREQUENCY = 2502.44100 Hz

SPEED OF SOUND = 1128.06500 ft/s  
 WAVE NUMBER = 13.93830 1/ft  
 SVD SINGULARITY FACTOR = 1.00000E-06

PRESSURE REFERENCE SENSOR DESIGNATION = 1  
 PRESSURE REFERENCE SPL = 139.895 dB

UPSTREAM -> DOWNSTREAM TRANSFER FUNCTION = 3.728600E-01 2.366900E-01

J	DSGN	X, in.	Y, in.	Z, in.	PTFReal	PTFImag	Std Dev
1	1	4.9450	4.0100	.0000	3.7286E-01	2.3669E-01	1.000
2	2	3.3500	4.0100	.0000	9.7359E-01	-2.2610E-02	1.000
3	3	1.6800	4.0100	.0000	9.6007E-01	8.3316E-03	1.000
4	4	.0700	4.0100	.0000	9.7068E-01	-4.0927E-02	1.000
5	5	.0000	2.0000	.0000	7.8031E-01	1.2724E-01	1.000
6	6	.0800	.0000	.0000	6.0176E-01	3.2300E-01	1.000
7	7	1.6750	.0000	.0000	5.0503E-01	3.2770E-01	1.000
8	8	3.3550	.0000	.0000	3.7452E-01	2.7852E-01	1.000
9	9	4.9450	.0000	.0000	3.3511E-01	2.4029E-01	1.000
10	10	5.0000	2.0000	.0000	6.6886E-01	1.1296E-01	1.000
11	11	3.9450	4.0100	1.0100	7.2577E-01	6.0812E-01	1.000
12	12	3.3500	4.0100	1.0100	7.9223E-01	6.0589E-01	1.000
13	13	1.6800	4.0100	1.0100	7.7074E-01	6.3769E-01	1.000
14	14	.0700	4.0100	1.0100	7.5216E-01	7.2881E-01	1.000
15	15	.0000	2.0000	1.0100	2.8012E-01	6.9952E-01	1.000
16	16	.0800	.0000	1.0100	-2.2964E-01	6.7099E-01	1.000
17	17	1.6750	.0000	1.0100	-2.6726E-01	5.7291E-01	1.000
18	18	3.3550	.0000	1.0100	-2.7713E-01	5.1069E-01	1.000
19	19	4.9450	.0000	1.0100	-2.9167E-01	4.4999E-01	1.000
20	20	5.0000	2.0000	1.0100	2.0044E-01	5.2798E-01	1.000

NUMBER OF MEASUREMENT POINTS = 20  
 NUMBER OF X-MODES = 4  
 NUMBER OF Y-MODES = 2

PROPAGATION CONSTANTS (1/ft - k-MULTIPLIED)  
 & AXIAL WAVELENGTH, inches F => Fwd, B => Bkwd

MX NY	RePKF	ImPKF	ZWLF	RePKB	ImPKB	ZWLB
1 1	13.938300	.000000	5.409	-13.938300	.000000	-5.409
1 2	10.268870	.000000	7.342	-10.268870	.000000	-7.342
2 1	11.722930	.000000	6.432	-11.722930	.000000	-6.432

2	2	6.971423	.000000	10.815	-6.971423	.000000	-10.815
3	1	.000000	5.754962	*****	.000000	-5.754962	*****
3	2	.000000	11.042920	*****	.000000	-11.042920	*****
4	1	-.000001	17.814720	*****	.000001	-17.814720	*****
4	2	-.000001	20.154170	*****	.000001	-20.154170	*****

MX	NY	FWD COL#	BKWD COL#
1	1	1	9
2	1	2	10
3	1	3	11
4	1	4	12
1	2	5	13
2	2	6	14
3	2	7	15
4	2	8	16

FOR SUCCESSFUL SVD, INFO SHOULD BE ZERO. INFO = 0

J,AWSV =	1	15.304210
J,AWSV =	2	13.798030
J,AWSV =	3	6.726806
J,AWSV =	4	5.581583
J,AWSV =	5	4.776353
J,AWSV =	6	4.434527
J,AWSV =	7	4.177710
J,AWSV =	8	3.927159
J,AWSV =	9	3.452292
J,AWSV =	10	2.945761
J,AWSV =	11	2.579583
J,AWSV =	12	2.309944
J,AWSV =	13	1.997982
J,AWSV =	14	1.502061
J,AWSV =	15	1.198104
J,AWSV =	16	9.730095E-01

WMAX = 1.5304E+01 WMIN = 1.5304E-05

MEASURED MODE COEFFICIENTS

FORWARD		COMPLEX COEFFICIENT		MAGNITUDE	PHASE, deg
MX	NY				
1	1	2.20887E-01	1.85616E-01	2.88521E-01	40.0409
1	2	-1.55600E-01	5.91786E-02	1.66473E-01	159.1769
2	1	2.14197E-02	2.10687E-02	3.00449E-02	44.5267
2	2	-1.52943E-03	3.38961E-02	3.39306E-02	92.5835
3	1	2.52804E-02	-6.83934E-03	2.61892E-02	-15.1384
3	2	-3.61784E-03	-1.83505E-03	4.05662E-03	-153.1048
4	1	1.99567E-03	-3.85673E-03	6.18741E-03	-71.1835
4	2	-9.07159E-04	3.08077E-03	3.21155E-03	106.4075

BACKWARD		COMPLEX COEFFICIENT		MAGNITUDE	PHASE, deg
MX	NY				
1	1	1.08770E-02	3.53515E-02	3.69869E-02	72.8979
1	2	2.16747E-02	-6.36685E-02	6.72568E-02	-71.1999
2	1	-4.26381E-03	-5.43283E-05	4.26416E-03	-179.2700
2	2	2.32581E-02	-7.75607E-03	2.45172E-02	-18.4424
3	1	-1.63557E-02	5.12006E-03	1.71384E-02	162.6175
3	2	5.43420E-03	1.48397E-03	5.63318E-03	15.2739
4	1	3.40208E-04	2.07723E-03	2.10490E-03	80.6987
4	2	-5.33287E-04	-1.39540E-04	5.51241E-04	-165.3367

MODE COEFFICIENT FIT STANDARD DEVIATIONS

J	StdDev
1	2.7423E-01
2	3.6430E-01
3	8.5133E-01
4	3.9004E-01
5	3.4790E-01
6	6.2362E-01
7	6.2393E-01

8 3.9481E-01  
 9 2.7423E-01  
 10 3.6430E-01  
 11 5.5608E-01  
 12 9.2672E-02  
 13 3.4790E-01  
 14 6.2362E-01  
 15 2.8592E-01  
 16 8.1578E-02

FORWARD ENERGY UPSTREAM = 2.5153E+00 WATTS

BACKWARD ENERGY UPSTREAM = -2.2421E-02 WATTS

FORWARD ENERGY DOWNSTREAM = 3.4217E-01 WATTS

BACKWARD ENERGY DOWNSTREAM = -1.6348E-02 WATTS

DELTA PWL = -8.6635E+00 dB

\*\*\*\*\*  
 NEXT MODE COMBINATION  
 \*\*\*\*\*

NUMBER OF MEASUREMENT POINTS = 20  
 NUMBER OF X-MODES = 2  
 NUMBER OF Y-MODES = 4

PROPAGATION CONSTANTS (1/ft - k-MULTIPLIED)  
 & AXIAL WAVELENGTH, inches F => Fwd, B => Bkwd

MX	NY	RePKF	ImPKF	ZWLF	RePKB	ImPKB	ZWLB
1	1	13.938300	.000000	5.409	-13.938300	.000000	-5.409
1	2	10.268870	.000000	7.342	-10.268870	.000000	-7.342
1	3	-.000001	12.689750	*****	.000001	-12.689750	*****
1	4	-.000001	24.600040	*****	.000001	-24.600040	*****
2	1	11.722930	.000000	6.432	-11.722930	.000000	-6.432
2	2	6.971423	.000000	10.815	-6.971423	.000000	-10.815
2	3	-.000001	14.760710	*****	.000001	-14.760710	*****
2	4	-.000001	25.729570	*****	.000001	-25.729570	*****

MX	NY	FWD COL#	BKWD COL#
1	1	1	9
2	1	2	10
1	2	3	11
2	2	4	12
1	3	5	13
2	3	6	14
1	4	7	15
2	4	8	16

FOR SUCCESSFUL SVD, INFO SHOULD BE ZERO. INFO = 0

J,AWSV = 1 23.047460  
 J,AWSV = 2 19.182560  
 J,AWSV = 3 10.500460  
 J,AWSV = 4 9.561220  
 J,AWSV = 5 4.556411  
 J,AWSV = 6 4.497321  
 J,AWSV = 7 4.267453  
 J,AWSV = 8 3.561482  
 J,AWSV = 9 3.476959  
 J,AWSV = 10 2.708364  
 J,AWSV = 11 1.844897  
 J,AWSV = 12 1.831978  
 J,AWSV = 13 8.316209E-07  
 J,AWSV = 14 5.038856E-07  
 J,AWSV = 15 4.465964E-07  
 J,AWSV = 16 1.335616E-07

WMAX = 2.3047E+01 WMIN = 2.3047E-05  
 J, SING AWSV= 13 8.3162E-07  
 J, SING AWSV= 14 5.0389E-07  
 J, SING AWSV= 15 4.4660E-07  
 J, SING AWSV= 16 1.3356E-07

MEASURED MODE COEFFICIENTS

FORWARD		COMPLEX COEFFICIENT		MAGNITUDE	PHASE, deg
MX	NY				
1	1	1.39222E-01	-2.72742E-01	3.06220E-01	-62.9578
1	2	-2.81917E-01	-1.00403E-01	2.99262E-01	-160.3970
1	3	-2.68390E-02	-1.80876E-02	3.23650E-02	-146.0228
1	4	-2.98804E-01	-6.86865E-02	3.06597E-01	-167.0542
2	1	-2.49721E-02	1.07919E-02	2.72042E-02	156.6279
2	2	9.34493E-03	-7.69038E-03	1.21025E-02	-39.4525
2	3	-6.39968E-03	-3.30033E-03	7.20056E-03	-152.7197
2	4	9.23154E-03	-7.99469E-03	1.22121E-02	-40.8932

BACKWARD		COMPLEX COEFFICIENT		MAGNITUDE	PHASE, deg
MX	NY				
1	1	-3.37953E-02	-2.66190E-03	3.38999E-02	-175.4964
1	2	-2.75279E-01	-4.15290E-02	2.78394E-01	-171.4210
1	3	7.78177E-03	2.10799E-03	8.06223E-03	15.1570
1	4	3.20010E-03	-1.02676E-01	1.02726E-01	-88.2148
2	1	-8.20181E-03	1.15759E-02	1.41870E-02	125.3185
2	2	8.96645E-03	-7.81149E-03	1.18919E-02	-41.0621
2	3	6.04235E-03	8.47101E-03	1.04052E-02	54.4999
2	4	8.29347E-03	-5.05687E-03	9.71358E-03	-31.3724

MODE COEFFICIENT FIT STANDARD DEVIATIONS

J	StdDev
1	3.0319E-01
2	3.5688E-01
3	1.2270E-01
4	1.5497E-01
5	4.7399E-01
6	4.7547E-01
7	1.3217E-01
8	1.7171E-01
9	3.0319E-01
10	3.5688E-01
11	1.2270E-01
12	1.5497E-01
13	1.6293E-01
14	1.3878E-01
15	4.9808E-02
16	6.3850E-02

NUMBER OF MEASUREMENT POINTS = 20  
 NUMBER OF X-MODES = 2  
 NUMBER OF Y-MODES = 4

PROPAGATION CONSTANTS (1/ft - k-MULTIPLIED)  
 & AXIAL WAVELENGTH, inches F => Fwd, B => Bkwd

MX	NY	RePKF	ImPKF	ZWLF	RePKB	ImPKB	ZWLB
1	1	13.938300	.000000	5.409	-13.938300	.000000	-5.409
1	2	10.268870	.000000	7.342	-10.268870	.000000	-7.342
1	3	-.000001	12.689750	*****	.000001	-12.689750	*****
1	4	-.000001	24.600040	*****	.000001	-24.600040	*****
2	1	11.722930	.000000	6.432	-11.722930	.000000	-6.432
2	2	6.971423	.000000	10.815	-6.971423	.000000	-10.815
2	3	-.000001	14.760710	*****	.000001	-14.760710	*****
2	4	-.000001	25.729570	*****	.000001	-25.729570	*****

MX	NY	FWD COL#	BKWD COL#
1	1	1	9
2	1	2	10
1	2	3	11

2	2	4	12
1	3	5	13
2	3	6	14
1	4	7	15
2	4	8	16

FOR SUCCESSFUL SVD, INFO SHOULD BE ZERO. INFO = 0

J,AWSV =	1	23.047460
J,AWSV =	2	19.182560
J,AWSV =	3	10.500460
J,AWSV =	4	9.561220
J,AWSV =	5	4.556411
J,AWSV =	6	4.497321
J,AWSV =	7	4.267453
J,AWSV =	8	3.561482
J,AWSV =	9	3.476959
J,AWSV =	10	2.708364
J,AWSV =	11	1.844897
J,AWSV =	12	1.831978
J,AWSV =	13	8.316209E-07
J,AWSV =	14	5.038856E-07
J,AWSV =	15	4.465964E-07
J,AWSV =	16	1.335616E-07

WMAX =	2.3047E+01	WMIN =	2.3047E-05
J, SING AWSV=	13	8.3162E-07	
J, SING AWSV=	14	5.0389E-07	
J, SING AWSV=	15	4.4660E-07	
J, SING AWSV=	16	1.3356E-07	

MEASURED MODE COEFFICIENTS

FORWARD		COMPLEX COEFFICIENT		MAGNITUDE	PHASE, deg
MX	NY				
1	1	2.26594E-01	1.87760E-01	2.94276E-01	39.6458
1	2	-4.07963E-02	1.53748E-03	4.08252E-02	177.8417
1	3	-5.79262E-03	3.75135E-03	6.90123E-03	147.0726
1	4	-4.01201E-02	5.42658E-03	4.04855E-02	172.2970
2	1	2.59220E-02	2.08156E-02	3.32452E-02	38.7648
2	2	6.59834E-03	9.62324E-03	1.16681E-02	55.5629
2	3	7.81686E-04	3.50984E-03	3.59583E-03	77.4444
2	4	8.06908E-03	9.88569E-03	1.27608E-02	50.7774

BACKWARD		COMPLEX COEFFICIENT		MAGNITUDE	PHASE, deg
MX	NY				
1	1	1.11513E-02	3.10205E-02	3.29640E-02	70.2274
1	2	-3.62688E-02	6.19348E-03	3.67938E-02	170.3093
1	3	1.79593E-03	-1.25379E-03	2.19029E-03	-34.9201
1	4	-1.62818E-02	-1.77365E-02	2.40766E-02	-132.5513
2	1	-7.27442E-03	-2.84364E-03	7.81047E-03	-158.6490
2	2	7.94985E-03	8.39731E-03	1.15635E-02	46.5679
2	3	-1.22202E-03	-1.39147E-03	1.85190E-03	-131.2902
2	4	-1.46421E-03	-6.05460E-04	1.58446E-03	-157.5346

MODE COEFFICIENT FIT STANDARD DEVIATIONS

J	StdDev
1	3.0319E-01
2	3.5688E-01
3	1.2270E-01
4	1.5497E-01
5	4.7399E-01
6	4.7547E-01
7	1.3217E-01
8	1.7171E-01
9	3.0319E-01
10	3.5688E-01
11	1.2270E-01
12	1.5497E-01
13	1.6293E-01
14	1.3878E-01

15 4.9808E-02  
16 6.3850E-02

FORWARD ENERGY UPSTREAM = 5.2287E-01 WATTS

BACKWARD ENERGY UPSTREAM = -1.9061E-01 WATTS

FORWARD ENERGY DOWNSTREAM = 2.8947E-01 WATTS

BACKWARD ENERGY DOWNSTREAM = -7.1766E-03 WATTS

DELTA PWL = -2.5680E+00 dB

---

Other than the particular modes used in the expansion, the output from the two versions of the program provides the same information in the same format.

## **8. Appendix B - Calibration of the Acoustic Data Acquisition System**

### **8.1 Introduction**

The acoustic data acquisition system consists of 20 upstream transducers, 20 downstream transducers for Insertion Loss measurements and 2 transducers for the In-Situ Impedance measurements. The signals from the 20 upstream transducers (numbered 1 through 20) pass through VESHAY amplifiers (numbered 1 through 20) and are recorded on digital tape recorder METRUM #1.

Similarly, the signals from the 20 downstream transducers (numbered 21 through 40) pass through VESHAY amplifiers (numbered 21 through 40) and are recorded on METRUM #2 tape recorder. The signals from the two transducers for the In-Situ measurements pass through two PACIFIC amplifiers and are recorded on one of the above METRUM tape recorders. For on-line data reduction and analysis, 8 of the upstream signals and 8 of the downstream signals are fed to the 16 channel SD9000 analyzer. Also the signals from the two In-Situ transducers are fed to the PC based 2 channel analyzer for on-line computation of the impedance of test panels.

The calibration procedure described below is designed to correct acoustic data for channel to channel differences and for converting the signal amplitudes to dB levels.

### **8.2 Calibration of the Signal Conditioning Amplifiers and the Tape Recorder Systems**

For the calibration of the amplifiers and the tape recorder systems, set VESHAY gain to 100 and follow the steps described below.

1. Apply white noise signal source to VESHAY #1 through #20
2. Record calibration data on METRUM recorder #1
3. Apply white noise signal source to VESHAY #21 through #40
4. Record calibration data on METRUM recorder #2
5. If VESHAY #1 is replaced for any reason, repeat steps A and B. If VESHAY #21 is replaced for any reason, repeat steps C and D
6. If a VESHAY from #2 through #20 is replaced, apply white noise signals to VESHAY #1 and the new VESHAY and record the signals on the METRUM #1
7. If a VESHAY from #22 through #40 is replaced, apply white noise signals to VESHAY #21 and the new VESHAY and record the signals on the METRUM #2

### **8.3 Relative Calibration of the Kulite Transducers**

For the following steps, set each VESHAY gain to 1000.

1. Install the “reference Kulite” transducer in position #1 of the calibration tube and connect it to VESHAY #1.
2. Install up to 4 Kulite transducers in positions #2 through #5 of the calibration tube and connect them to VESHAYs #2 through #5 respectively.
3. Apply white noise signal to the calibration speaker and record the data on METRUM #1.

#### **8.4 Amplitude Calibration**

For the following steps, set each VESHAY gain to 1000.

1. Apply a discrete frequency Piston Phone signal (250 Hz., 120 dB) to the “reference transducer and record the data on METRUM #1.
2. Install the “reference Kulite” transducer in position #1 of the calibration tube and connect it to VESHAY #1.
3. Install up to 4 Kulite transducers in positions #2 through #5 of the calibration tube and connect them to VESHAYs #2 through #5 respectively.
4. Apply discrete frequency 250 Hz signal to the calibration speaker and record the data on METRUM #1.

#### **8.5 Relative and Amplitude Calibration of the Transducers, Signal Conditioning Amplifiers, and the Tape Recorder System**

For the following steps, set the gain for each SPECIFIC and VESHAY amplifier to 1000.

1. Install the “reference Kulite” transducer in position #1 of the calibration tube and connect it to VESHAY #1.
2. Install the In-Situ Kulites #1 and #2 in positions #2 and #3 of the calibration tube and connect them to PACIFIC #1 and PACIFIC #2 respectively.
3. Connect VESHAY #1 to channel #1 and PACIFIC #1 and PACIFIC #2 to channels 21 and 22 of METRUM #1 (or METRUM #2 if necessary).
4. Apply white noise signal to the calibration speaker and record the data.
5. Apply discrete signal at 250 Hz to the calibration speaker and record the data.

The above calibration data will be reduced and applied, during the reduction of recorded test data as described in Appendix C.

## 9. Appendix C - Procedure for the Reduction of the Flow Duct Acoustic Data

### 9.1 Introduction

The acoustic data acquisition system for the insertion loss measurements (by the modal decomposition method) consists of two arrays with 20 transducers in each array.

The upstream transducer array consists of 20 Kulite transducers (numbered 1 to 20), connected to channels 1 through 20 of the digital tape recorder METRUM #1 through the signal conditioning amplifiers VESHAY #1 through #20.

The downstream transducer array also consists of 20 Kulite transducers (numbered 1 to 20), connected to channels 1 through 20 of the digital tape recorder METRUM #2 through the signal conditioning amplifiers VESHAY #21 through #40.

The procedures described below show how to reduce the recorded calibration and test data. All recorded data is to be reduced in the frequency range 0 to 10kHz with a bandwidth between 10 and 20 Hz.

### 9.2 Relative Calibrations Of A Transducer Array System

The transducer array system consists of 20 Kulites, 20 Veshay amplifiers and a Metrum tape recorder.

The relative calibration correction for a transducer channel #i relative to the transducer channel #1 is defined as the transfer function  $X_c(i,1,f)$ , obtained when both transducer systems are subjected to the same acoustic pressure input in a calibration tube. This transfer function is given by

$$X_c(i,1,f) = \{S(i,f).S^*(1,f)\} / \{S(1,f).S^*(1,f)\} = X_s(i,1,f) . X_t(i,1,f) \quad (1)$$

where  $f$  is the acoustic frequency,  $X_s(i,1,f)$  is the relative correction of the “system” channels (without transducers) consisting of the amplifiers, the tape recorder channels and the Analyzer’s A-D converter channels.  $X_t(i,1,f)$  is the relative correction of the  $i^{\text{th}}$  and the  $1^{\text{st}}$  transducers.

The calibration data were recorded in accordance with the procedures described in Appendix B. The data reduction procedures are described below.

Suffixes “u” and “d” are used below to refer to the upstream and downstream transducer systems.

### 9.2.1 Relative Calibrations $X_{S_u}(i, 1, f)$ Of The Upstream Systems

The upstream systems consist of Veshay Amplifiers #1 through 20, the Metrum #1 tape recorder and the SD9000 analyzer.

Execute the following steps to reduce the recorded data:

- A. Connect output channels 1 through 16 of METRUM #1, to input channels 1 through 16 of the SD9000 respectively.
- B. Play back white noise data recorded per section 1.2, steps A and B of Appendix B and analyze to obtain the time averaged values (frequency domain averaging) of the following transfer function data

$$X_{S_u}(i, 1, f) = \{S_u(i, f) \cdot S_u^*(1, f)\} / \{S_u(1, f) \cdot S_u^*(1, f)\}$$

where  $i = 2, 3, 4, 5, \dots, 16$ .

- C. Connect output channels 1, 17, 18, 19 and 20 of METRUM #1, to input channels 1, 2, 3, 4 and 5 of the SD9000 respectively.
- D. Play back white noise data recorded per section 1.2, steps A and B of Appendix B and analyze to obtain the time averaged values (frequency domain averaging) of the following transfer function data

$$X_{S_u}(i+16, 1, f) = \{S_u(i, f) \cdot S_u^*(1, f)\} / \{S_u(1, f) \cdot S_u^*(1, f)\}$$

where  $i = 2, 3, 4$  and  $5$ .

### 9.2.2 Relative Calibrations $X_{S_d}(i, 1, f)$ Of The Downstream Systems

The downstream system consists of Veshay amplifiers #21 through 40, the Metrum #2 tape recorder & the analyzer SD9000.

Execute the following steps to reduce the recorded data:

- A. Connect output channels 1 through 16 of METRUM #2, to input channels 1 through 16 of the SD9000 respectively.
- B. Play back white noise data recorded per section 1.2, steps C and D of Appendix B and analyze to obtain the time averaged values (frequency domain averaging) of the following transfer function data

$$X_{S_d}(i, 1, f) = \{S_d(i, f) \cdot S_d^*(1, f)\} / \{S_d(1, f) \cdot S_d^*(1, f)\}$$

where  $i = 2, 3, 4, 5, \dots, 16$ .

- C. Connect output channels 1, 17, 18, 19 and 20 of METRUM #2, to input channels 1, 2, 3, 4 and 5 of the SD9000 respectively.
- D. Play back white noise data recorded per section 1.2, steps C and D of Appendix B and analyze to obtain the time averaged values (frequency domain averaging) of the following transfer function data

$$X_{S_d(i+16,1,f)} = \{S_d(i,f) \cdot S_d^*(1,f)\} / \{S_d(1,f) \cdot S_d^*(1,f)\}$$

where  $i = 2, 3, 4$  and  $5$ .

### 9.2.3 The Calibration Of The Transducers Relative To A Reference Transducer

The relative calibration data for the Kulite transducers were recorded per the instructions in Section 8.3 of Appendix B. All data were recorded using VESHAY amplifiers # 1, 2, 3, 4 and 5 on tracks 1 through 5 of METRUM #1. A reference transducer was connected to VESHAY #1. Transducers #  $n$ ,  $(n+1)$ ,  $(n+2)$  and  $(n+3)$  were connected to VESHAY #2 through 5.

#### 9.2.3.1 Relative Calibration Of The 20 Upstream Transducers

Execute the following steps.

- A. Connect output channels 1 through 5 of METRUM #1 to input channels 1 through 5 of the SD9000 analyzer.
- B. Play back the relative calibration data for the upstream transducers #  $n$ ,  $(n+1)$ ,  $(n+2)$  and  $(n+3)$ , where  $n = 1$ . Analyze the data to obtain the time averaged values (frequency domain averaging) of the following transfer function data

$$X_{C_u(n,0,f)} = \{S(n,2,f) \cdot S^*(0,1,f)\} / \{S(0,1,f) \cdot S^*(0,1,f)\}$$

$$X_{C_u(n+1,0,f)} = \{S(n+1,3,f) \cdot S^*(0,1,f)\} / \{S(0,1,f) \cdot S^*(0,1,f)\}$$

$$X_{C_u(n+2,0,f)} = \{S(n+2,4,f) \cdot S^*(0,1,f)\} / \{S(0,1,f) \cdot S^*(0,1,f)\}$$

$$X_{C_u(n+3,0,f)} = \{S(n+3,5,f) \cdot S^*(0,1,f)\} / \{S(0,1,f) \cdot S^*(0,1,f)\}$$

Note: in the term  $S(x, y, f)$ ,  $x$  represents the transducer number,  $y$  represents the A-D channel number and  $f$  represents the frequency.

- C. Calculate the relative calibration data for the transducers #  $n$ ,  $(n+1)$ ,  $(n+2)$  and  $(n+3)$  as follows

$$X_{t_u}(n,0,f) = X_{c_u}(n,0,f) / X_{s_u}(2,1,f)$$

$$X_{t_u}(n+1,0,f) = X_{c_u}(n+1,0,f) / X_{s_u}(3,1,f)$$

$$X_{t_u}(n+2,0,f) = X_{c_u}(n+2,0,f) / X_{s_u}(4,1,f)$$

$$X_{t_u}(n+3,0,f) = X_{c_u}(n+3,0,f) / X_{s_u}(5,1,f)$$

D. Repeat steps B and C with  $n=5$ ,  $n=9$  and  $n=13$ .

We should now have transducer calibrations  $X_{t_u}(i,0,f)$ ;  $i=1, 2, 3, 4, \dots, 20$ ; for all the upstream transducers relative to the reference transducer.

### 9.2.3.2 Relative Calibration Of The 20 Downstream Transducers

Execute the following steps.

- A. Connect output channels 1 through 5 of METRUM #1 to input channels 1 through 5 of the SD9000 analyzer.
- B. Play back the relative calibration data for the downstream transducers #  $n$ ,  $(n+1)$ ,  $(n+2)$  and  $(n+3)$ , where  $n = 1$ . Analyze the data to obtain the time averaged values (frequency domain averaging) of the following transfer function data

$$X_{c_d}(n,0,f) = \{S(n,2,f) \cdot S^*(0,1,f)\} / \{S(0,1,f) \cdot S^*(0,1,f)\}$$

$$X_{c_d}(n+1,0,f) = \{S(n+1,3,f) \cdot S^*(0,1,f)\} / \{S(0,1,f) \cdot S^*(0,1,f)\}$$

$$X_{c_d}(n+2,0,f) = \{S(n+2,4,f) \cdot S^*(0,1,f)\} / \{S(0,1,f) \cdot S^*(0,1,f)\}$$

$$X_{c_d}(n+3,0,f) = \{S(n+3,5,f) \cdot S^*(0,1,f)\} / \{S(0,1,f) \cdot S^*(0,1,f)\}$$

Note: in the term  $S(x, y, f)$ ,  $x$  represents the transducer number,  $y$  represents the A-D channel number and  $f$  represents the frequency.

- C. Calculate the relative calibration data for the transducers #  $n$ ,  $(n+1)$ ,  $(n+2)$  and  $(n+3)$  as follows

$$X_{t_d}(n,0,f) = X_{c_d}(n,0,f) / X_{s_d}(2,1,f)$$

$$X_{t_d}(n+1,0,f) = X_{c_d}(n+1,0,f) / X_{s_d}(3,1,f)$$

$$X_{t_d}(n+2,0,f) = X_{c_d}(n+2,0,f) / X_{s_d}(4,1,f)$$

$$X_{td}(n+3,0,f) = X_{cd}(n+3,0,f) / X_{sd}(5,1,f)$$

D. Repeat steps B and C with  $n=5$ ,  $n=9$  and  $n=13$ .

We should now have transducer calibrations  $X_{td}(i,0,f)$ ;  $i=1, 2, 3, 4, \dots, 20$ ; for all the downstream transducers relative to the reference transducer.

#### 9.2.4 Calculation Of The Total System Relative Calibrations

We have reduced the relative calibration data in sections 2.2.1, 2.2.2 and 2.2.3 to obtain the following relative calibration data:

- $X_{su}(i,1,f)$  ; the relative calibrations of the upstream amplifiers, VESHAY #1 through #20, connected to the input channels #1 through #20 of tape recorder METRUM #1. No transducers were included during this calibration. These calibrations are with respect to the upstream data channel #1.
- $X_{sd}(i,1,f)$  ; the relative calibrations of the downstream amplifiers, VESHAY #21 through #40, connected to the input channels #1 through #20 of tape recorder METRUM #2. No transducers were included during this calibration. These calibrations are with respect to the upstream data channel #1.
- $X_{tu}(i,0,f)$  ; the relative calibrations of the 20 upstream Kulite transducers with respect to a reference transducer #0.
- $X_{td}(i,0,f)$  ; the relative calibrations of the 20 downstream Kulite transducers with respect to a reference transducer #0.

As during the test, transducer #1 is connected to the data channel #1, we have to determine “total channel calibration correction”, using equation (1), as follows :

$$X_{cu}(i,1,f) = X_{su}(i,1,f) \cdot X_{tu}(i,0,f) / X_{tu}(1,0,f)$$

$$X_{cd}(i,1,f) = X_{sd}(i,1,f) \cdot X_{td}(i,0,f) / X_{td}(1,0,f)$$

where the data channel number,  $i = 1, 2, 3, 4, 5, \dots, 20$ . The calibrations,  $X_{cu}(i,1,f)$  and  $X_{cd}(i,1,f)$ , will be used in correcting the reduced test data from the upstream and the downstream data channels.

### 9.3 Reduction And Correction Of The Transducer Signals

This applies to the 20 upstream and 20 downstream transducer signals recorded on tape recorders Metrum #1 and Metrum #2, respectively.

All recorded data will be reduced in the frequency range 0 to 10 kHz with the same setup that was used for the reduction of the calibration data. These data will be reduced using the “signal enhancement method” (time domain averaging).

#### 9.3.1 Reduction Of The Recorded Data From The Up Stream Transducers

Execute the following steps to reduce the upstream data.

- A. Connect output channels #1 through 16 of METRUM #1 recorder to input channels 1 through 16 of the SD9000 analyzer.
- B. Replay the recorded test data, starting at a specified value of the IRIG time code, and reduce to obtain the following time averaged transfer function data

$$Hm_u(i, 1, f) = \{S(i, f) \cdot S^*(1, f)\} / \{S(1, f) \cdot S^*(i, f)\}$$

and the auto spectral value  $\{S(1, f) \cdot S^*(1, f)\}$   
where  $i = 2, 3, 4, 5, \dots, 16$ ;  $f$  is the acoustic excitation frequency.

- C. Connect output channels #1, #17, #18, #19 and #20 of METRUM #1 recorder to input channels 1 through 5 of the SD9000 analyzer.
- D. Replay the recorded test data, starting at the specified value of the IRIG time code used in step B above, and reduce to obtain the following time averaged transfer function data

$$Hm_u(i+16, 1, f) = \{S(i, f) \cdot S^*(1, f)\} / \{S(1, f) \cdot S^*(i, f)\}$$

where  $i = 2, 3, 4$  and 5.

- E. Compute the corrected transfer function data as follows:

$$Hc_u(i, 1, f) = Hm_u(i, 1, f) / Xc_d(i, 1, f)$$
$$SPL_u(1, f) =$$

for  $i = 2, 3, 4, 5, \dots, 20$ .

#### 9.3.2 Reduction Of The Recorded Data From The Downstream Transducers

Execute the following steps to reduce the downstream data.

- A. Connect output channels #1 through 16 of METRUM #2 recorder to input channels 1 through 16 of the SD9000 analyzer.
- B. Replay the recorded test data, starting at a specified value of the IRIG time code (used in the reduction of upstream data), and reduce data to obtain the following time averaged transfer function data

$$H_{m_d}(i, 1, f) = \{S(i, f) \cdot S^*(1, f)\} / \{S(1, f) \cdot S^*(1, f)\}$$

and the auto spectral value  
 $\{S(1, f) \cdot S^*(1, f)\}$   
 where  $i = 2, 3, 4, 5, \dots, 16$ ;  $f$  is the acoustic excitation frequency.

- C. Connect output channels #1, #17, #18, #19 and #20 of METRUM #2 recorder to input channels 1 through 5 of the SD9000 analyzer.
- D. Replay the recorded test data, starting at the specified value of the IRIG time code used in step B above, and reduce to obtain the following time averaged transfer function data

$$H_{m_u}(i+16, 1, f) = \{S(i, f) \cdot S^*(1, f)\} / \{S(1, f) \cdot S^*(1, f)\}$$

where  $i = 2, 3, 4$  and 5.

- E. Compute the corrected transfer function data as follows:

$$H_{c_d}(i, 1, f) = H_{m_d}(i, 1, f) / X_{c_d}(i, 1, f)$$

$$SPL_d(1, f) =$$

for  $i = 2, 3, 4, 5, \dots, 20$ .

## 10. Appendix D - DC Flow Resistance and Impedance Measurements with Grazing Flow

### 10.1 Measurement of Impedance with Grazing Flow by the Two-Microphone Method

Attempts at the in-situ measurement of impedance in the presence of grazing flow using the two-microphone method were generally unsuccessful, for all instrumented panels. The duct test treatment panel instrumented for the grazing flow measurement is shown schematically in Volume 3 in Figure 2.2-2. Figure 10.1 is an illustration of the method of mounting the two microphones in a treatment panel hexcell.

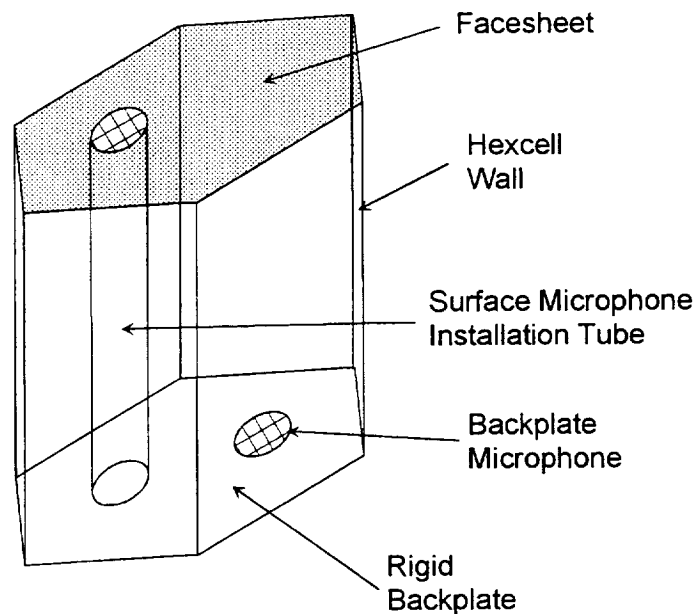


**Figure 10.1 Illustration of microphone installation in hexcell cavity for in-situ two-microphone grazing flow impedance measurement method.**

A check of the measurement technique in a rigid wall cavity showed excellent correlation of measured data with theory. This check was performed before setting up the panels in the Flow Duct. The impedance with broad band excitation at Mach 0.0 was designed to check the quality of test location in the panel. If the measurement looked reasonable then "good data" would be expected under grazing flow conditions. Unfortunately, the checks were unsatisfactory for all the four panels. Due to the questionable validity of the results, no impedance measurement data is presented.

The principal reason for the problem is suspected to be the transmission of sound through hexcell cavity walls. A second possibility is a problem with the seal at the bond between the facesheet and the particular hexcell chosen for the impedance measurement. Although extreme

care was taken in the fabrication of these panels, it is difficult to insure that each individual hexcell is properly sealed. Apparently an unlucky choice of cell to instrument was made on four separate occasions.

One method of possibly preventing this problem is to insert a rigid-walled tube into the back of the treatment panel after cutting out a core plug, as shown in Figure 10.2. Special care in fabrication would be required to seal the tube against the facesheet. The tube need not be the same depth as the honeycomb, and, in fact, tubes of several different lengths could be installed for different frequency ranges. The two microphones would be installed through a rigid backplate at the end of the tube. The smaller tube holding the microphone that is to be located at the faceplate could be used as a guide to drill a hole in the faceplate through which the microphone could be inserted and aligned with the faceplate surface.

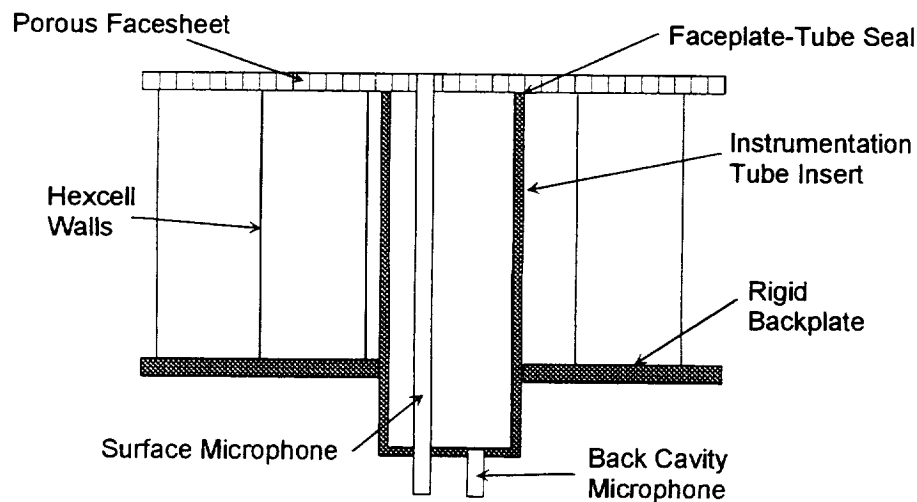


**Figure 10.2** Diagram of proposed improved two-microphone impedance measurement method.

Although the two-microphone in-situ impedance measurement with grazing flow has been accomplished successfully in the past by numerous researchers, it is questionable whether improvements in the method are worth pursuing for application to scaled treatment designs. The problems in measurement will be compounded by the increased precision required to make the measurement at higher frequencies, particularly considering the smaller hexcell cross-dimension required. Other methods of measuring impedance in the presence of grazing flow at high frequencies are likely to hold more promise, and their development would be a better investment of resources than attempting to improve the two-microphone method.

## 10.2 DC Flow Tests with Grazing Flow

### 10.2.1 The Test Apparatus

These tests were conducted in the 4 inch by 5 inch rectangular flow duct apparatus. This test apparatus is schematically illustrated in Figure 10.3 below. A schematic drawing of the test panel instrumented with the DC flow feature is shown in Volume 3, Figure 2.2-2.

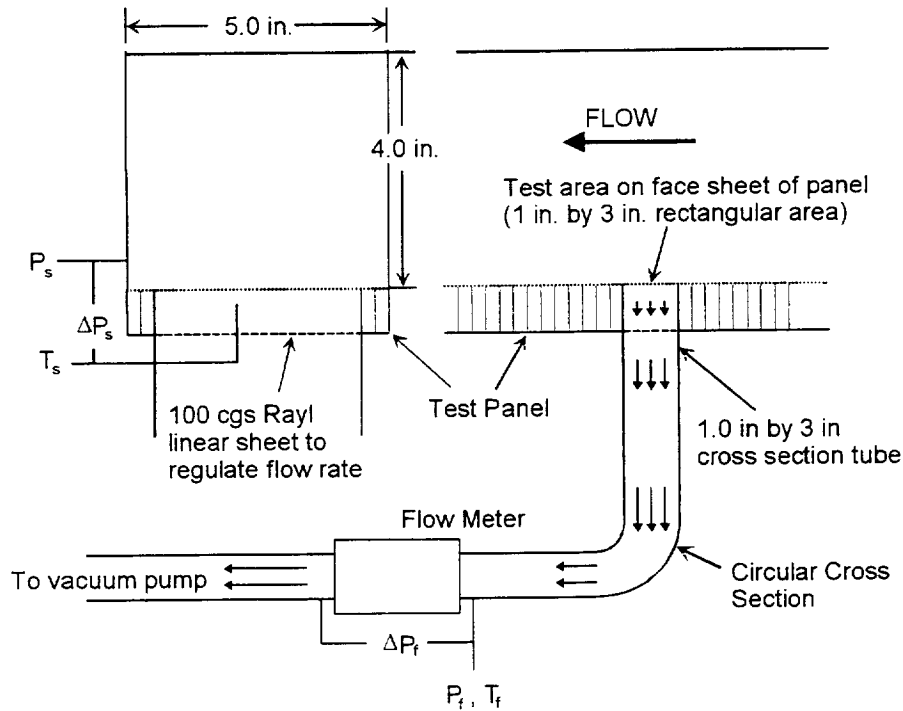


**Figure 10.3** Diagram of the DC flow resistance with grazing flow apparatus installation in the grazing flow duct.

The DC flow test area is built into the single-degree-of-freedom test panel. The air sucked through the sample flowed into a tube with a 1.0 in. by 3.0 in cross section at the top and a circular cross section at the bottom. A laminar flow element Meriam flow meter with maximum flow rate of 20 SCFM was used to measure the flow rates. A needle valve was also employed downstream of the flow meter to control air flow through the test area.

Validyne pressure transducers were used to measure the pressures  $P_s$ ,  $\Delta P_s$ ,  $P_f$ , and  $\Delta P_f$ . The pressure transducers were calibrated with the help of a Druck Model 601 digital pressure indicator with the labeled uncertainty of 1% full scale. The Druck was calibrated by the Evendale Standards Lab on the established cycles, by a traceable standard to an accuracy of 0.05% full scale. A thermocouple was used to measure the temperature of the air downstream of the sample. The temperature of the flow in the DC flow apparatus was assumed to be constant.

Great care was taken to eliminate any leakages in the apparatus between the test panel and the flow meter. This was necessary to ensure measurement accuracy. There are, however, some anomalies in the data which suggest possible leaks in the “sample region” of the panels.

### 10.2.2 Test Data

DC flow resistance measurements in the presence of grazing flow were made on four different instrumented panels, as indicated in Table 10.1, below. The measurements were made at Mach 0.0, 0.2, 0.3, 0.4, 0.5, 0.6, 0.7, and 0.8 in the GEAE Flow Duct Facility.

Panel Designation	Treatment Description	Scale	Faceplate POA or Resistance	Cavity Depth, in.
1.1.2	PP SDOF	FULL	10%	1.0
1.2.1	PP SDOF	HALF	10%	0.5
1.3.1	PP SDOF	PP 1/5 DPTH 1/2	10%	0.5
4.2	LINEAR SDOF	FULL	90 Rayl	1.0

**Table 10.1 List of panels instrumented for DC flow resistance with grazing flow measurement.**

The measured data were fit to the standard linear form for DC flow resistance as a function of through-flow velocity,

$$R_{DC} = A + BU \quad (10.-1)$$

where A is the intercept and B is the slope obtained from a linear curve-fit to the measured data.

Three plots are presented for each panel in Figures 10.4 to 10.15. The first plot in each group of three shows the measured DC flow resistance data for all of the flow Mach numbers. The second plot shows the curve fit for the intercept (A-value) as a function of Mach number. The third plot shows the slope (B-value) as a function of Mach number.

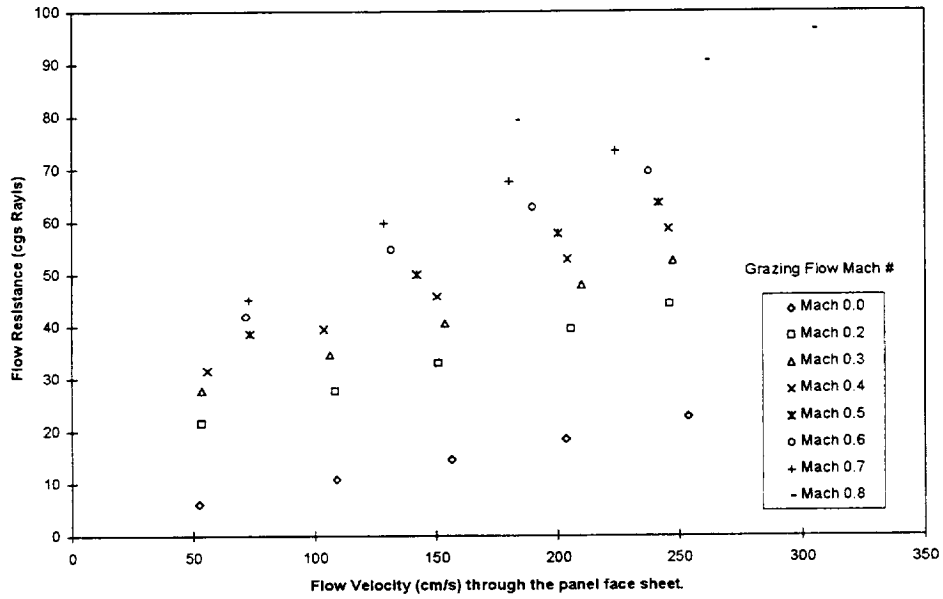


Figure 10.4 DC flow resistance data measured for Panel 1.1.2 in the presence of grazing flow.

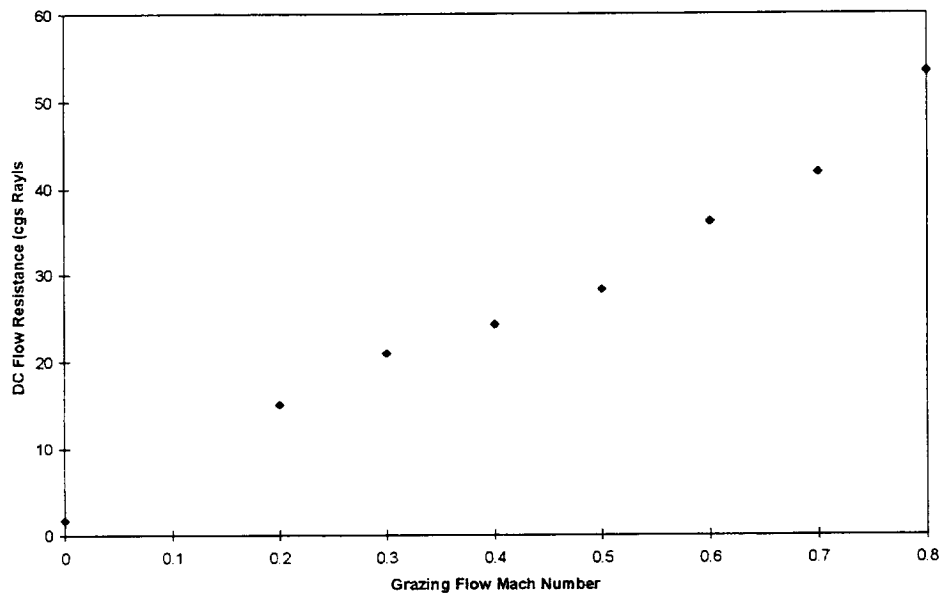


Figure 10.5 Variation of DC flow resistance “intercept” value with grazing flow Mach number for Panel 1.1.2

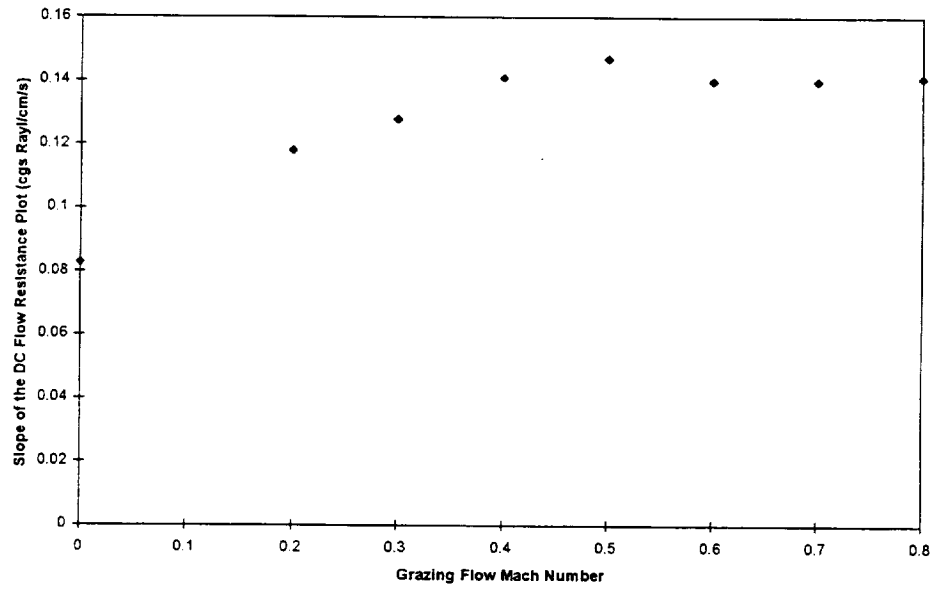


Figure 10.6 Variation of DC flow resistance “slope” with grazing flow Mach number for Panel 1.1.2.

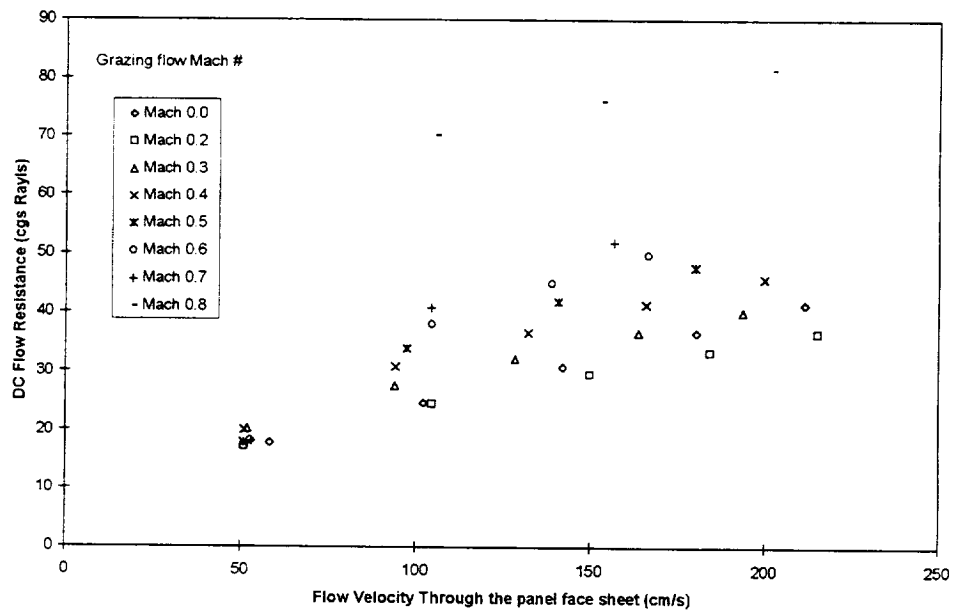


Figure 10.7 DC flow resistance data measured for Panel 1.2.1 in the presence of grazing flow.

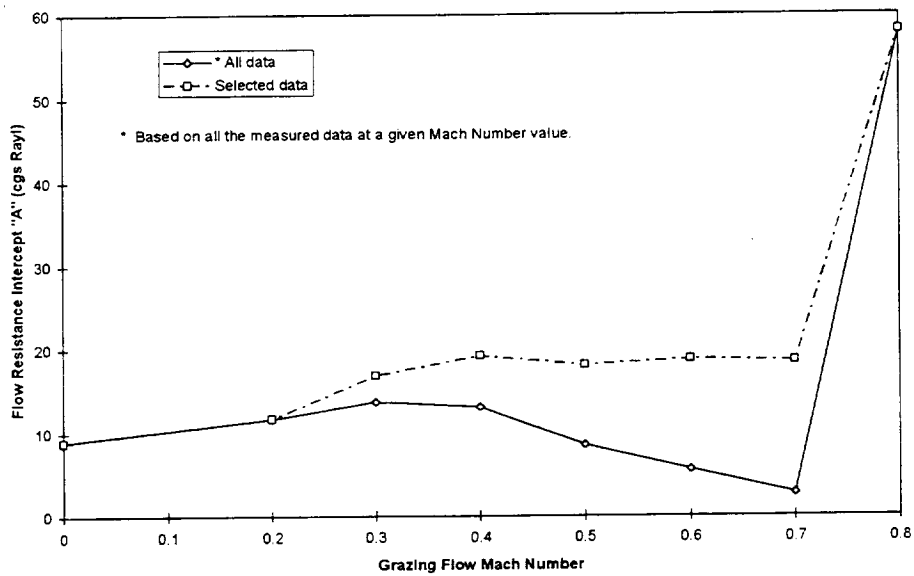


Figure 10.8 Variation of DC flow resistance “intercept” value with grazing flow Mach number for Panel 1.2.1

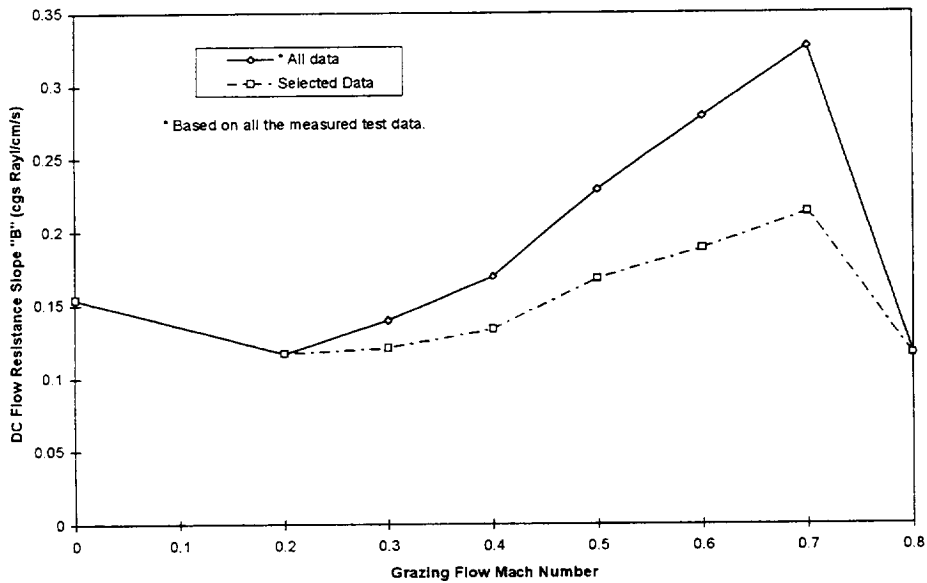


Figure 10.9 Variation of DC flow resistance “slope” with grazing flow Mach number for Panel 1.2.1.

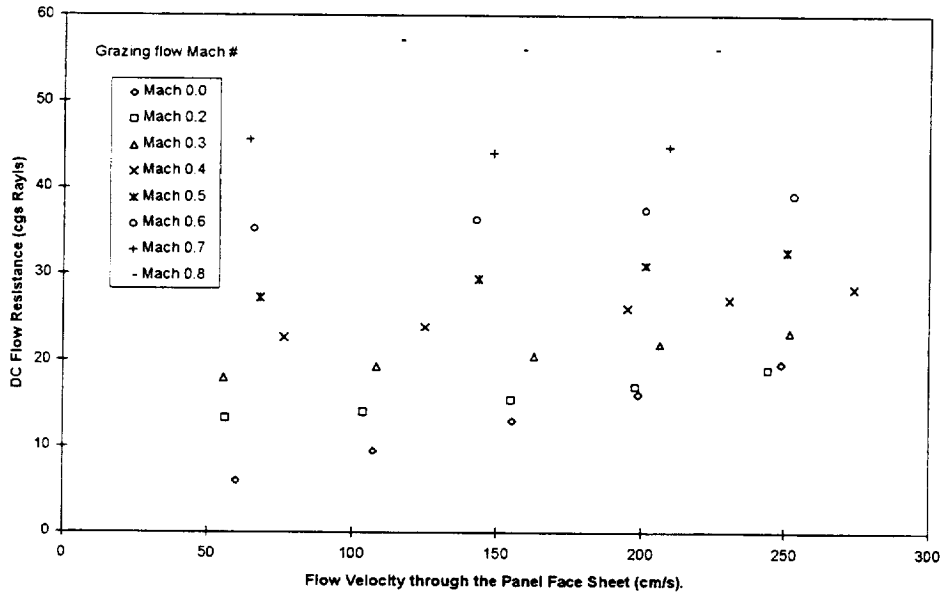


Figure 10.10 DC flow resistance data measured for Panel 1.3.1 in the presence of grazing flow.

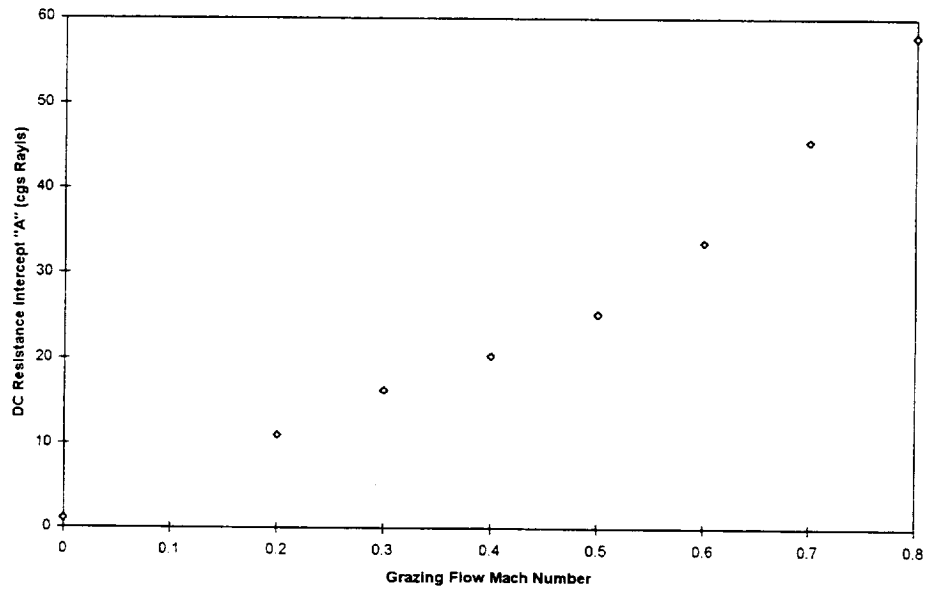


Figure 10.11 Variation of DC flow resistance "intercept" value with grazing flow Mach number for Panel 1.3.1

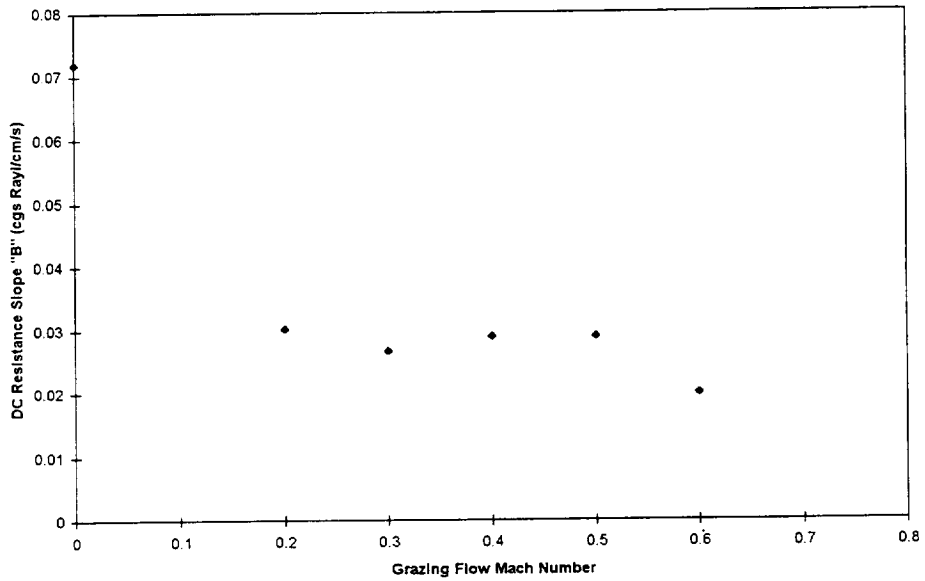


Figure 10.12 Variation of DC flow resistance "slope" with grazing flow Mach number for Panel 1.3.1.

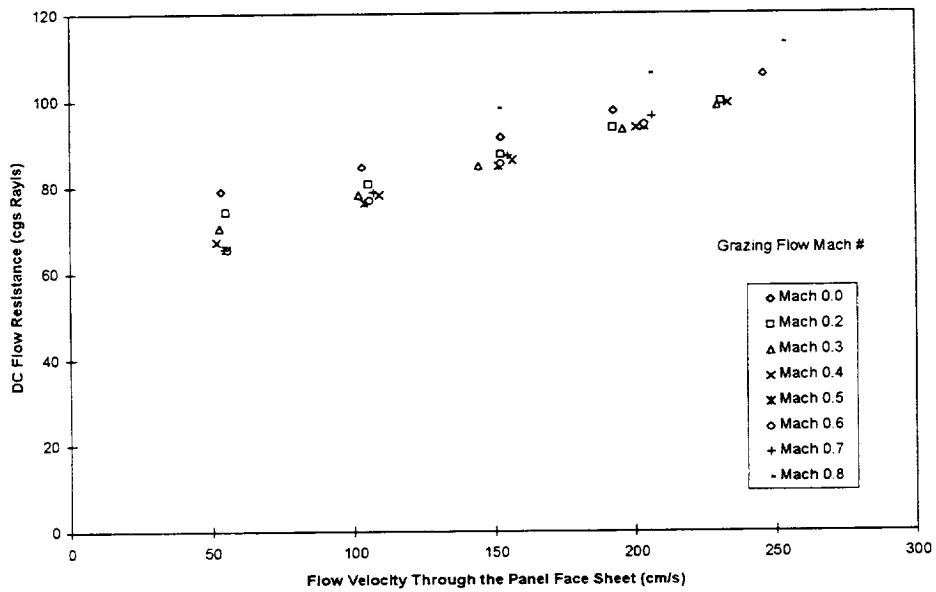


Figure 10.13 DC flow resistance data measured for Panel 4.2 in the presence of grazing flow.

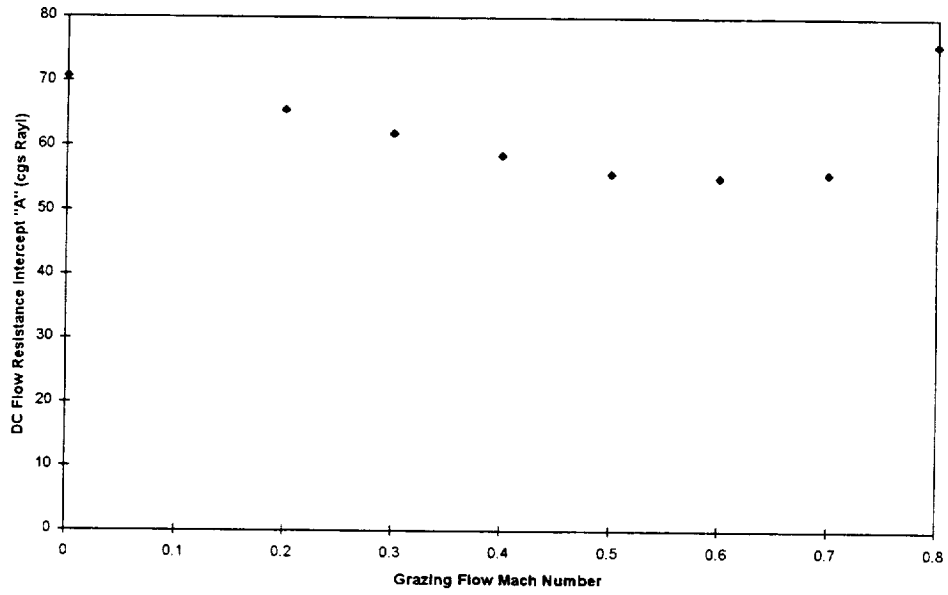


Figure 10.14 Variation of DC flow resistance “intercept” value with grazing flow Mach number for Panel 4.2

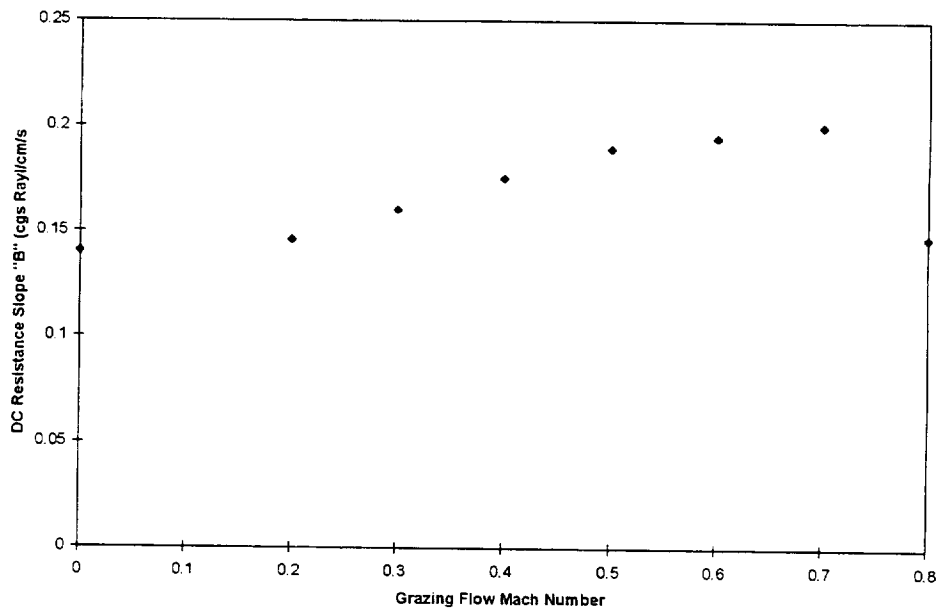


Figure 10.15 Variation of DC flow resistance “slope” with grazing flow Mach number for Panel 4.2.

The results for Panel 1.2.1 in Figures 10.7, 10.8, and 10.9 indicate a measurement problem, suspected to be caused by a defective panel sample. These results should be ignored, but are included to indicate the nature of the data when measurement problems are experienced.

The results for the two perforated plate panels show expected behavior as a function of grazing flow Mach number, where the linear part of the flow resistance, the intercept  $A$ , increases approximately linearly with Mach number, except possibly for a slightly more rapid increase as Mach 0.8 is approached. Panel 1.1.2 is a full scale facesheet, with 0.039 inch hole diameter and 0.025 inch thickness, while Panel 1.3.1 is a 1/5 scale facesheet, with 0.008 inch hole diameter and 0.005 inch thickness. For Panel 1.1.2, the nonlinear part, the slope  $B$ , increases up to about Mach 0.5, and then levels off. The  $B$ -value for the 1/5 scale Panel 1.3.1 decreases with Mach number, going to zero at about Mach 0.7.

The wiremesh facesheet, Panel 4.2, shows less sensitivity of both  $A$ -value and  $B$ -value to grazing flow, as might be expected. The  $A$ -value, as shown in Figure 10.14, drops slowly with Mach number up to about Mach 0.65, then seems to increase rapidly. The  $B$ -value shows a slow increase up to about Mach 0.7, then drops.

DC flow resistance measurements with grazing flow, performed with care and using carefully instrumented panels, show promise as a useful method for obtaining information about flow effects on the resistance of facesheets, even up to Mach numbers of 0.8. Use of these tests in the future and further correlation of the data with analytical models is highly recommended.

